Australian Government
Department of the Environment and Energy
Supervising Scientist

internal report 626

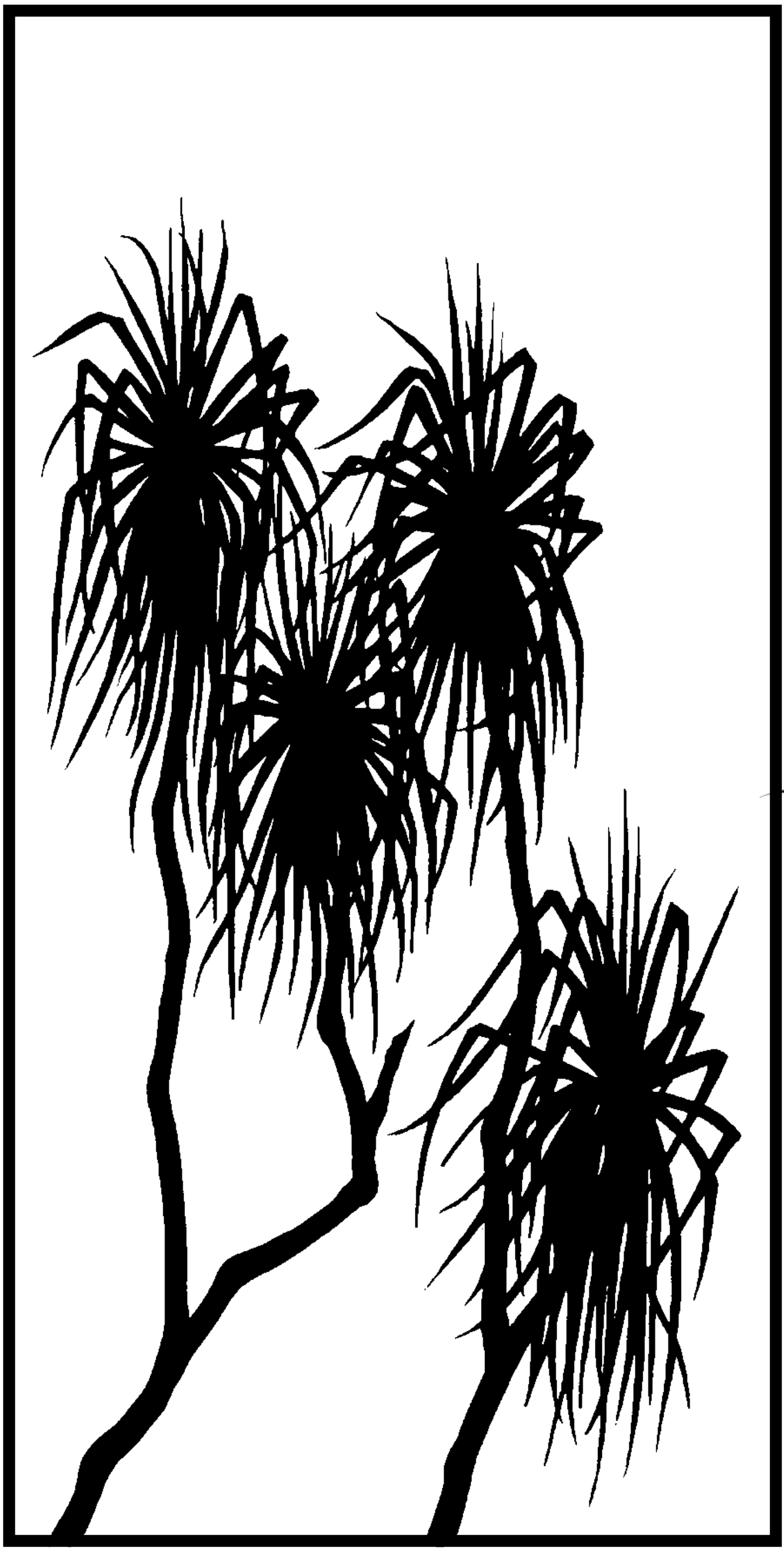

Water quality and biota in the subsurface sands of Magela Creek – report of a pilot project

Lisa Chandler, Moya Tomlinson

& Chris Humphrey

November 2017

Release status – Unrestricted

The Department acknowledges the traditional owners of country throughout Australia and their continuing connection to land, sea and community. We pay our respects to them and their cultures and to their elders both past and present.

Water quality and biota in the subsurface sands of Magela Creek – report of a pilot project

Lisa Chandler, Moya Tomlinson & Chris Humphrey

Supervising Scientist
GPO Box 461, Darwin NT 0801

November 2017

(Release status – Unrestricted)

Australian Government
Department of the Environment and Energy
Supervising Scientist

How to cite this report:

Chandler L, Tomlinson M, Humphrey C. 2017. Water quality and biota in the subsurface sands of Magela Creek – report of a pilot project.

Project number: RES-2016-004

Authors of this report:

Lisa Chandler –Supervising Scientist, GPO Box 461, Darwin NT 0801, Australia
Chris Humphrey –Supervising Scientist, GPO Box 461, Darwin NT 0801, Australia
Moya Tomlinson - Supervising Scientist, GPO Box 461, Darwin NT 0801, Australia

Supervising Scientist is a branch of the Australian Government Department of the Environment and Energy.

Supervising Scientist
Department of the Environment and Energy
GPO Box 461, Darwin NT 0801 Australia

environment.gov.au/science/supervising-scientist/publications

Disclaimer

Contents

Acknowledgments

Associate Professor Grant Hose (Macquarie University) is thanked for his advice and assistance in the field with the initial site set up in July.

The following SSB staff are thanked for their assistance with fieldwork: Royce Namarnyilk, Mitchel Rudge, Tom Mooney, Ceiwen Pease, Costi Buccella, and Andrew Harford.

We greatly appreciate the advice on analyses, and insight, comments and suggestions of Dr David Jones.

Executive summary

This report presents results from a pilot project carried out in 2016 to investigate the water quality and biota in the subsurface saturated sands of the Magela Creek sand channel. The study commenced in the dry season, after the creek had ceased to flow, following the 2015-16 wet season.

Magela Creek, a seasonal tributary of the East Alligator River, flows through the Ranger mine Project Area and lies immediately adjacent to the mine site. Following closure of the Ranger uranium mine in 2026, the rehabilitated site is predicted to become a source of both contaminated surface water runoff and exfiltrating groundwater with elevated electrical conductivity (EC).

In 2015, an ecological risk assessment carried out by the Supervising Scientist Branch (Supervising Scientist 2017) identified the following key knowledge needs:

1) What is the source, extent (longitudinal, lateral, depth), rate of movement and residence times of current mine solute contamination in the subsurface dry season flows in Magela sand channel downstream of Ranger, are there impacts associated with this contamination and how might this information inform knowledge needs for closure?
2) What is the composition and extent of hyporheic and stygofauna communities?

In July 2016, temporary piezometers were installed to approximately 1.5 m depth at 12 sites along the western channel of Magela Creek from upstream to downstream of the Ranger mine site. Site selection was informed by preliminary water quality sampling in June 2016. Data loggers (CTD-Divers) were deployed in each piezometer to record temperature and EC at 10-minute intervals. In each piezometer in July and August 2016, field water quality variables (pH, EC, and temperature) were recorded and groundwater fauna sampled using a plankton net. Water chemistry samples were also collected from selected sites for analysis of metals, ions and nutrients. Subsequent sampling was not possible due to an unseasonal rain event and stream flow in September 2016 which damaged some piezometers and required retrieval of the data loggers. This rain event resulted in flow in Magela Creek which, in the ensuing five weeks, receded until cessation of flow on 25th October.

The continuous data showed that the groundwater EC upstream of Ranger (MCMB01) was relatively stable, with a median of 41 μS cm^{-1} until the creek flowed in September, dropping to 8 μS cm^{-1} then slowly increasing as the surface water levels receded. EC in the mid-reach series of four piezometers displayed peaks, reaching a maximum of 566 μS cm^{-1} on the 19th September when surface flow commenced. The high EC in this mid-reach series of piezometers for the duration of the study was indicative of mine water contamination, as it was associated with high concentrations of Mg and SO_4. Some peaks were associated with rainfall events, but others were unexplained and could indicate the passage of a localised pulse of contaminated water. In the mid-reach, EC dropped significantly (21 μS cm^{-1}) when flow commenced, but rose quickly once the surface water levels dropped. EC in some piezometers at the outlet of mine water-contaminated Coonjimba Billabong (CJBB) increased significantly after rain in early September, possibly indicating a preferential groundwater flow path out of CJBB. Peaks may also be associated with mobilisation of contaminants in groundwater sourced from historical land application areas (LAAs) adjacent to CJBB.

Water chemistry analysis indicated the high EC values were associated with high concentrations of Mg and SO_4, as well as other contaminants of potential concern (COPCs) associated with mine activities (ie Mn, U). Principal components analysis showed the most influential gradients were

associated with higher concentrations of Mg and SO_4 that separated the sites near CJBB from other 'reference.'

Despite the limited number of faunal samples, the results establish the presence of a groundwater community in the subsurface saturated sands of Magela Creek. Excluding taxa of terrestrial origin, a total of 144 individuals from 13 taxa were collected. Nematodes, oligochaete worms and harpacticoid copepods were the most abundant taxa. A number of specimens of Syncarida, tentatively identified as members of the family Parabathynellidae, were collected. Australian parabathynellids have been found to be quite diverse with restricted distributions and therefore are of particular conservation significance. The specimens collected from Magela Creek are potentially a new record for the Northern Territory.

This pilot project identified the need for further work in the following areas:

- Further sampling of biota in the sand channel, including genomic characterisation;
- More extensive water chemistry sampling, spatially and seasonally;
- Construction of deeper bores to sample biota and investigate the extent of contamination beyond the 3.6 m limit of the sampling equipment;
- Expansion of the sampling to other streams, for example Gulungul Creek Tributary 2, where there is an existing contamination gradient and a similar uncontaminated small stream, Gulungul Creek and reference sites in Nourlangie and Burdulba Creeks, to better determine landscape scale patterns of groundwater fauna in alluvial sand sediments of the Alligator Rivers Region.
- Investigation of the sources of chemical contamination of the Magela Creek sand channel. (Potential sources are Coonjimba Billabong and/or the adjacent Djalkmara LAA);
- Improving understanding of the behaviour of the solute contamination within the sand channel following dilution by surface water during flow events in the wet season in relation to the rapid elevation of EC levels observed as water levels dropped after creek flow commenced in September during the pilot project;
- Determination of the sensitivity of biota to COPCs, using both existing contaminant gradients and laboratory testing of whole organisms and/or genomic characterisation of exposed substrates.

1 Introduction

1.1 Study site

The Alligator Rivers Region (ARR), east of Darwin is renowned for its rich cultural and natural heritage and includes the World-Heritage listed Kakadu National Park (KNP). The Ranger uranium mine is located within KNP and to ensure protection of the environment, the Federal Government operates the Supervising Scientist Branch (SSB) (of the Department of the Environment and Energy) which carries out supervision, monitoring and research associated with uranium mining activities in the ARR. Magela Creek, a seasonal tributary of the East Alligator River, flows through the Ranger mine Project Area in close proximity to Pit 3 (Figure 1).

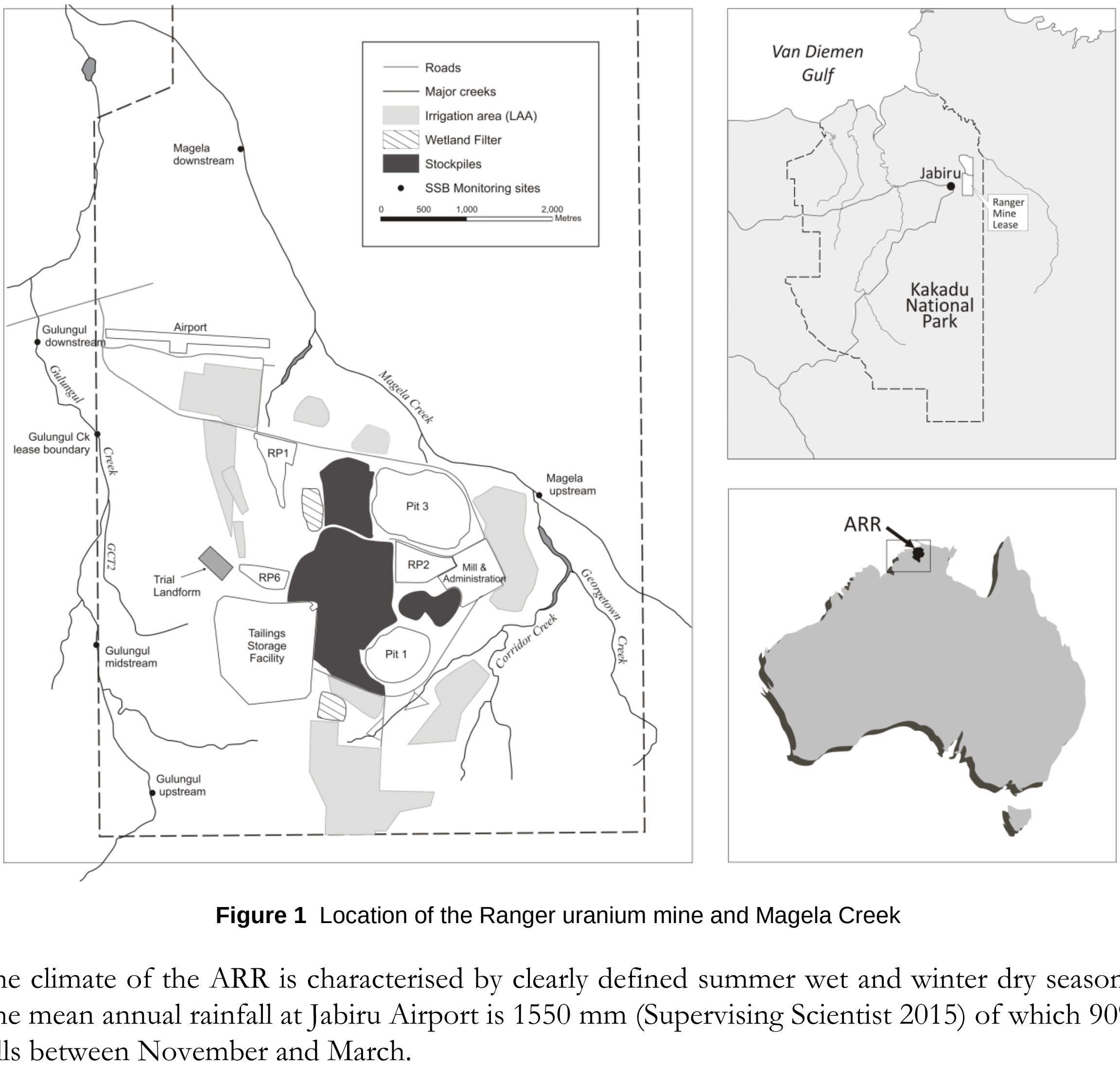

Figure 1 Location of the Ranger uranium mine and Magela Creek

The climate of the ARR is characterised by clearly defined summer wet and winter dry seasons. The mean annual rainfall at Jabiru Airport is 1550 mm (Supervising Scientist 2015) of which 90% falls between November and March.

Magela Creek catchment covers 1600 km^2, 26% of which is on the Arnhem Land plateau composed predominantly of resistant Kombolgie Formation sandstone (Nanson et al 1993). Between the plateau escarpment and Mudginberri Billabong (12 km downstream of the Ranger mine), Magela Creek is an anastomosing sand-bed channel with flow divided around large intrachannel vegetated islands stabilised by dense root mats of shrub and tree species including *Pandanus aquaticus*, *Lophopetalum arnhemicum*, *Syzygium* spp. and *Melaleuca* spp. (Jansen & Nanson 2004).

The sand channel has been filled since the Holocene with medium-coarse sands with an average particle diameter of 450 μm (Roberts 1991). Average thickness (depth of sand to original stream bed) has been reported as 5-6 m by Ahmad et al (1982) and 8-12 m by Nanson et al (1993). However a recent literature review indicated the sand channel could be much deeper (P Baker pers comm). The difference in reported thicknesses is likely to be related to longitudinal location along the creek; Roberts (1991) described the upper 6 km of the sand channel (ie below the escarpment or ~15 km upstream of Ranger) as less than 100 m wide and 5 m deep, and the lower 24 km as broadening to 100-300 m wide and deepening to 7-11 m. Magela Creek flows out onto an expansive clay-based lowland floodplain that covers 200 km^2 (Pettit et al 2011).

Surface waters of Magela Creek are characterised as slightly acidic, with low EC, low alkalinity and low concentrations of suspended solids, major ions, trace elements and radionuclides (Noller 1991).

Surface flow in Magela Creek ceases for several months during the dry season (approximately June to October). Early wet season flow is not observed in Magela Creek adjacent to Ranger until after approximately 200 mm of rainfall has occurred in the upper catchment area (Leaney & Puhalovich 2006), indicating that a period of recharge to the near-surface sand-bed is required before flow is expressed at the surface. The water table in the sand channel is at an average depth of 0.6 m below the deepest depressions at the end of the dry season (Ahmad et al 1982). Flow exceeds bankfull discharge for an average of 40 days annually (Jansen & Nanson 2004). Peak wet season flows provide hydrological connectivity between stream channels, riparian zones and floodplains, transporting nutrients, sediments, organic matter and biota (Warfe et al 2011). After cease to flow, pools may persist throughout the dry season, maintained by longitudinal subsurface flow (Ahmad & Salas 1981).

1.2 Rationale for study

Following closure of the Ranger uranium mine in 2026, the rehabilitated site is predicted to become a source of both contaminated surface water runoff and exfiltrating groundwater with elevated electrical conductivity (EC). The major component of the elevated EC is magnesium sulfate ($MgSO_4$) derived from the waste rock landform and pit capping. Solute egress modelling predicts that within 10 years of closure, groundwater with Mg concentrations greater than the current chronic exposure limit (3 mg L^{-1}) will reach Magela Creek and that concentrations above this limit will remain for at least 10,000 years (ERA 2014). Note that this concentration does not take into account any potential dilution in the hyporheic zone[1] from mixing of groundwater with surface waters

There have been several occurrences of Mg contamination of the Magela Creek sand channel during the operational phase of the Ranger mine, resulting in higher than typical concentrations in the surface water or occurring outside the period of main creek flows. Efflorescence of $MgSO_4$ in the Magela Creek area was first noticed at the base of the Magela Creek LAA and on the creek banks in the 1993 dry season (Supervising Scientist for the Alligator Rivers Region 1994). EC in small residual pools in the creek bed in the affected area was much higher than in other pools (1450 μS cm^{-1} cf. 22 – 115 μS cm^{-1}), and pH was much lower (3.26 cf. 6.04 – 7.05) (Pidgeon & Boyden 1993). There has also been efflorescence of $MgSO_4$ in the Djalkmara LAA in 2007 and

---

[1] The hyporheic zone is an active ecotone between the surface water and groundwater in a stream, where exchanges of water, nutrients, and organic matter occur in response to variations in discharge and bed topography and porosity (Boulton et al 1998)

2009, resulting in an estimated Mg concentration of 5.4 mg L^{-1} entering Magela Creek and 6 mg L^{-1} entering Coonjimba Billabong due to transport during first flush.

In 2014, several EC events (ie exceedances above the surface water compliance value) with elevated levels of Mg and SO_4 were observed in Gulungul Creek, primarily associated with flushing of solutes from Gulungul Creek Tributary 2 (GCT2). (GCT2 is a small tributary flowing from the western wall of the Ranger Tailings Storage Facility, Figure 1.) The 72 hour chronic EC Limit was exceeded on 7 April 2014 in the western-most channel of Magela Creek downstream of its confluence with Gulungul Creek, due to input of high EC water from Gulungul Creek (Supervising Scientist 2015).

Aquatic fauna occur in a wide range of groundwater habitats, but sampling efforts have been patchy and it is likely that the true extent of biodiversity and distribution of groundwater fauna (stygofauna) in Australia is undocumented (Tomlinson & Boulton 2010). In tropical Australia, survey effort has mainly been associated with mining developments in the Pilbara region (Eberhard et al 2005). The only published records of stygofauna in the Northern Territory are of a parabathynellid syncarid from a bore on Newhaven Station (Cho et al 2006), an amphipod, atyid shrimp and a copepod from caves near Katherine (Bruce 1992, Dumont & Maas 1985, Moulds & Bannick 2012, Williams 1964), and of undescribed hyporheic fauna in Magela Creek (Paltridge et al 1997).

During the dry season and when there are no longer surface waters, there is a reported resident fauna in the dry and moist surface sands of Magela Creek. Through re-wetting experiments, Paltridge et al (1997) observed invertebrates in the top 20 cm of the sands that were a mix of (i) dormant taxa commonly observed in the surface waters and associated benthos, as well as (ii) groundwater (presumably obligate) specialists (ie stygofauna). This potential pool of invertebrates was expected to be collected in the 2016 pilot study.

Stygofauna are particularly sensitive to groundwater environment disturbance because they are adapted to near steady-state environment conditions and have very narrow spatial distributions (Hose et al 2015). Changes to environmental conditions, such as those predicted to occur in the Magela Creek sand channel after closure, could be considered a threat to stygofauna.

To date, little is known of the groundwater ecology of Magela Creek, nor of the potential impacts of elevated Mg concentrations and other COPCs on resident biological communities.

In the latter part of 2015 the Supervising Scientist Branch carried out an ecological risk assessment which identified the following key knowledge needs (KKNs) regarding groundwater ecosystems in the region (Supervising Scientist 2017):

1) What is the source, extent (longitudinal, lateral, depth), rate of movement and residence times of current mine solute contamination in the subsurface dry season flows in Magela sand channel downstream of Ranger, are there impacts associated with this contamination, and how might this information inform knowledge needs for closure?

2) What is the composition and extent of hyporheic and stygofauna communities?

This report presents results from a pilot project carried out in 2016 to investigate the water quality and biota in the subsurface saturated sands of the Magela Creek sand channel.

1.3 Preliminary investigations

In December 2015, sampling of subsurface water and pools identified elevated EC and/or magnesium in Magela Creek approximately 5 km downstream of Ranger uranium mine (MCDW and MCUSGC) (Figure 2). At the time it was hypothesised that subsurface contamination at this distance represented a pulse of mine-derived waters whose travel time and distance reached corresponded to a minesite source from the previous wet season.

Further work examining the water chemistry of pools, was undertaken in June 2016 to determine potential sampling sites for this pilot project. The June investigation located several pools with obvious precipitation of iron oxyhydroxides (Figure 3), elevated EC and low pH values (Table 1) in the western channel of Magela Creek immediately adjacent to Coonjimba Billabong (Figure 3). The site with the highest EC recorded (409 µS cm^{-1}) also had elevated levels of Mg, Mn and SO_4 (Table 1).

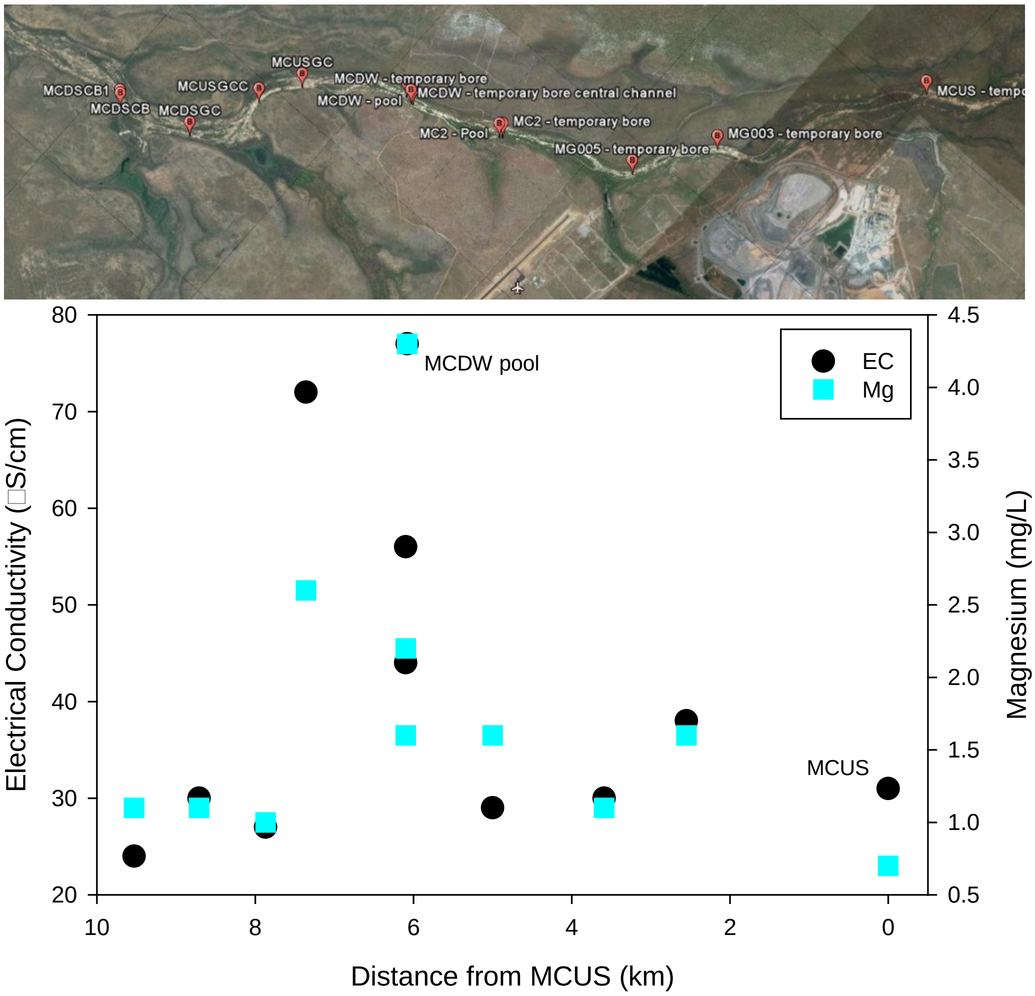

Figure 2 EC and Mg in Magela Creek pools or subsurface saturated sands (~0.7 m depth) in December 2015. Graph showing distance from upstream site (MCUS), with sites indicated on map above.

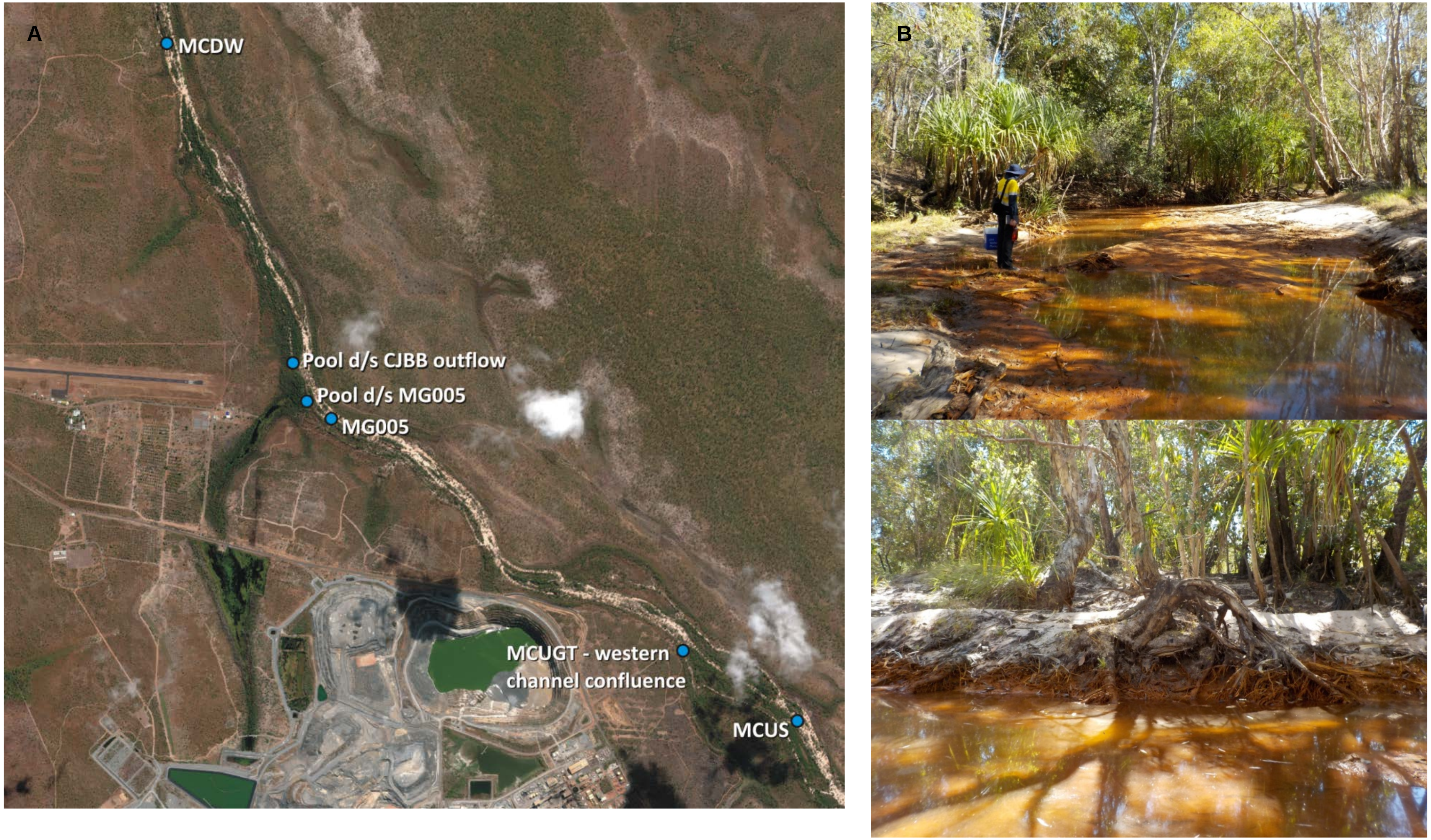

Figure 3 (A) Map of the pools sampled in June 2016 (B) Images of pool downstream of MG005 showing precipitation of iron oxyhydroxides.

Table 1 Water chemistry results from the June 2016 pool sampling. See Figure 3 for site locations

Site	**EC**	**pH**	**Filtered analytes**				
	(µS cm^{-1})		**Mg (mg L^{-1})**	**SO$_4$ (mg L^{-1})**	**Fe (µg L^{-1})**	**Mn (µg L^{-1})**	**U (µg L^{-1})**
MCUS	22	5.32	1	<0.1	38	85.8	0.004
MCUGT - western channel confluence	18	4.57	0.9	0.3	438	43	0.029
MG005	24	6.25	1.3	0.1	*708*[1]	62.6	0.025
Pool d/s MG005	409	3.07	17.8	124	64000	422	0.039
Pool d/s Coonjimba Billabong outflow	128	4.11	5.5	37.8	66	138	0.006
MCDW	25	5.94	1.2	0.3	134	26	0.028

1 MG005 duplicate sample had significantly lower concentrations of filtered Fe (44 µg L^{-1}). Total Fe results for the MG005 samples were the same however (1900 µg L^{-1})

Detailed spatial characterisation is required to determine the extent of these elevated solute concentrations, and to determine whether it is seasonal only, or indicative of long-term residency along the creek channel and through the sand depth profile. Characterisation of the subsurface fauna in the sands is also required for impact and risk assessment. Information arising from a study of current contamination should inform assessment of risks associated with groundwater expression of contaminants in Magela Creek predicted from Pit 3 closure modelling.

1.4 Objectives

There were two primary objectives for this dry season pilot study:

1) To characterise subsurface water quality in Magela Creek, improving understanding of the location and movement of current mine-water contamination in the creek, and
2) To determine the composition of groundwater communities.

The primary output for this project in 2016-17 was an indication of presence and composition of invertebrate communities of Magela Creek sand channel, and of dry season surface and subsurface water quality. The pilot will inform a more detailed sampling program to be undertaken in 2017-18 and following years that may also include Nourlangie and Gulungul Creeks and sampling of existing monitoring/operational bores on the Ranger mine Project Area for groundwater fauna.

2 Methods

2.1 Site selection and piezometer installation

In July 2016, temporary PVC piezometers were installed at 12 sites (Table 2) along the western channel of Magela Creek from upstream to downstream of the Ranger mine site (Figure 4). Sites were selected based on the results of the June survey (Table 1), with further refinement of sites around Coonjimba Billabong achieved by excavating a number of temporary holes and measuring the EC of the subsurface water.

Enviroequip 50 mm, 1.5 m PVC Bore casings and screens (Thermofisher Scientific) were used for the piezometers. The casing and screens were connected with threaded ends to create a 3 m piezometer (Figure 5). The screens are slotted along the length at 4 mm intervals with 0.5 mm wide slots. Using a picket driver, the screen was installed to a depth that ensured the slotted section of the piezometer would remain submerged despite any drop in subsurface water level as the dry season progressed; and the piezometer join was below the surface of the sand-bed. At some sites the installed depth was limited by the difficulty in driving the piezometer into the sand-bed. Both ends of the piezometers were capped.

In July two groups of existing bores were discovered in the central channel of Magela Creek (Figure 6, Line 1 and Line 2 in Table 2). A number of these bores, particularly at the first site (Bores1a-h - Figure 6a), had suffered fire damage, and/or had missing caps. Those without obvious damage could be useful for future work, but examination with a borehole camera is recommended to determine whether the integrity of these bores has been breached. These sites are believed to be those established in 1981 for a streambed underflow study (Ahmad et al 1982).

Table 2 Magela Creek monitoring bore details. Datum is WGS84

Bore ID	Short ID	Latitude	Longitude	Depth (m)[a]	Slotted interval (m)	Casing type
MCMB01	MB1	-12.67862906	132.93740256	1.57	1.5	50 mm CL18 uPVC
MCMB02	MB2	-12.66983194	132.91954388	1.59	1.5	50 mm CL18 uPVC
MCMB03	MB3	-12.65957559	132.90816859	1.76	1.5	50 mm CL18 uPVC
MCMB04	MB4	-12.65897699	132.90789736	1.63	1.5	50 mm CL18 uPVC
MCMB05	MB5	-12.65902492	132.90824671	1.74	1.5	50 mm CL18 uPVC
MCMB06	MB6	-12.65843405	132.90780976	1.60	1.5	50 mm CL18 uPVC
MCMB07	MB7	-12.65742611	132.90720134	1.22	1.5	50 mm CL18 uPVC
MCMB08	MB8	-12.65298626	132.90573740	1.29	1.5	50 mm CL18 uPVC
MCMB09	MB9	-12.64750542	132.90291072	1.53	1.5	50 mm CL18 uPVC
MCMB10	MB10	-12.64435347	132.90088419	1.67	1.5	50 mm CL18 uPVC
MCMB11	MB11	-12.64109521	132.90027581	1.82	1.5	50 mm CL18 uPVC
MCMB12	MB12	-12.64431718	132.90086608	1.69	1.5	50 mm CL18 uPVC
Line 1[b]	Bores 1a-h	-12.652969	132.906465	2.39 – 8.55	unknown	50 mm and 100 mm PVC with steel screens
Line 2[b]	Bores 2a-e	-12.658947	132.908441	4.79 - 5.34	unknown	50 mm and 100 mm PVC with steel screens

[a] Depth calculated using total depth of piezometer minus the case height above ground.

[b] From Ahmad et al (1982)

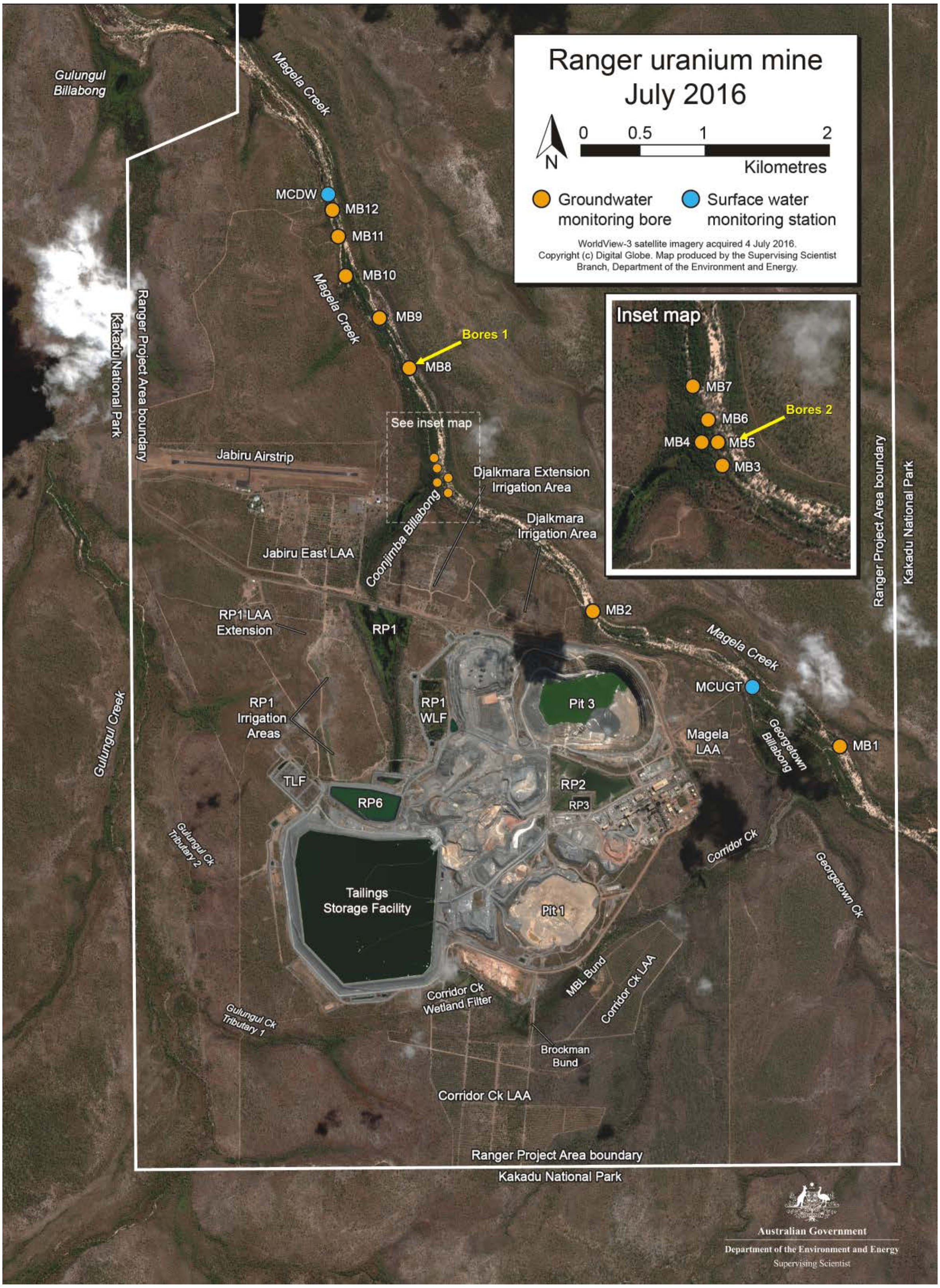

Figure 4 Map of piezometer sites.

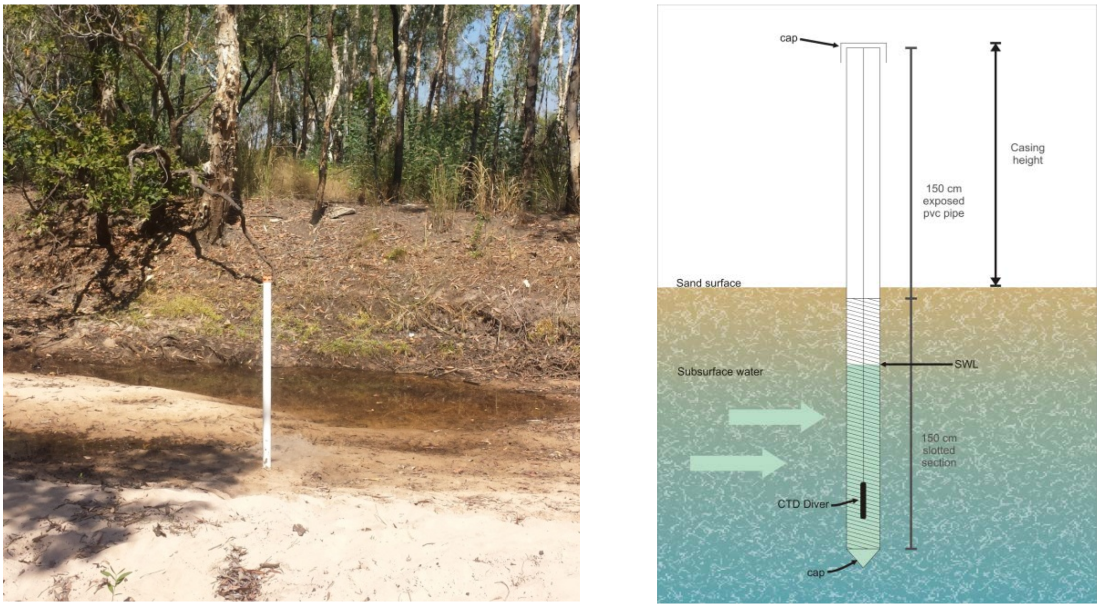

Figure 5 PVC piezometer design

Figure 6 Existing bores discovered in central Magela Creek channel, July 2016 (A) Bores 1a-h (Ahmad et al 1982; transverse 1, line 1) and (B) Bores 2a-e (Ahmad et al 1982; transverse 2, line 2)

2.2 Water Chemistry

Sampling was not possible after August 2016 due to an unseasonal rain event in September 2016. Subsequent creek flow inundated the piezometers and made site access difficult. Data loggers were retrieved when the creek water level dropped sufficiently in early October 2016, but no further sampling could be carried out.

2.2.1 Continuous data

Data loggers (CTD-Divers) were deployed in each piezometer to record temperature and EC at 10 minute intervals (Figure 5b indicates the relative position of the CTD-Divers). These data were retrieved from the CTD-Divers during each site visit, and uploaded into the Hydstra database.

2.2.2 Water quality determined from analysis of grab samples

Field-measured water quality variables (pH, EC and temperature) were recorded, using a Hydrolab minisonde (MS5), within each piezometer. The sonde was lowered to just above the bottom of the piezometer and measurements of field variables were collected both prior to purging and at the end of the site visit. This was done to determine whether there was any difference between the standing water in the piezometer and the surrounding groundwater.

In July, water chemistry samples were collected using an AMS "Piezometer Groundwater Sampling Kit" (AMS Inc., Figure 7). The kit consists of a 37.15 cm stainless steel slotted section with a #50 mesh screen, connected to up to four 91.44 cm stainless steel extensions; all with an inside diameter of 2.2 cm. This kit enabled discrete samples to be collected from deeper within the sand channel than the PVC piezometers allowed. Two samples were collected with this kit, one at the top of the subsurface water level, similar to the PVC piezometers (approximately 1 m), and one at the maximum depth reached by the AMS kit (approximately 3.6 m). In August water chemistry samples were only collected from the PVC piezometers (ie shallower depth), as the sampling kit was unavailable due to servicing requirements.

Figure 7 AMS Piezometer Groundwater Sampling Kit. Includes stainless steel slotted section with four extensions, allowing samples to be collected to a depth of 3.6 m

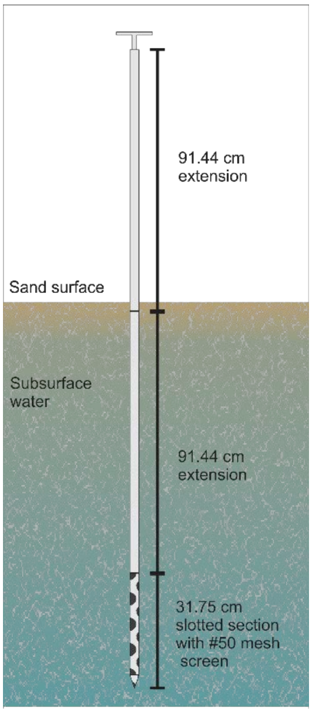

To ensure that the groundwater sample was representative of the water in the sand channel, three casing volumes were removed, as recommended by (Sundaram et al 2009), using a Geopump Series II peristaltic DC pump (Geotech Environmental Equipment, Inc). The pump speed was set low to reduce the draw down within the piezometer. This was performed when sampling from the PVC piezometers and when using the AMS groundwater kit. Once the piezometer was purged, a 1 L volume of sample was collected in a pre-rinsed acid washed bottle for analysis of the full suite of water chemistry variables (see Table 3). A portion of this 1 L sample was immediately filtered in the field using a 150 mL, 0.45 µm Nalgene filter unit for filtered metals and major ions. The remaining sample was decanted into separate appropriate bottles for analysis of total metals, major ions and alkalinity. In August, samples were also collected for nutrient analysis and total and dissolved organic carbon (TOC/DOC). The chemistry samples were analysed by NATA-accredited laboratory Intertek (Darwin) using a combination of ICP-AES, ICP-MS and FIA methods. TOC/DOC samples were analysed in-house using the high-temperature combustion method 5310B[2], (TOC-VCSH, Shimadzu Scientific Instruments, Oceania Pty. Ltd, SD <0.1 mg L^{-1}, maximum CV of 2%).

Table 3 Variables measured at each site (not all variables were measured on each sampling occasion).

Category	Feature/Analyte	Units
Bore structure	Total Depth of Bore	m
	Depth to water	m
	Height of casing	m
Water chemistry variables – continuous	Electrical Conductivity	µS cm^{-1}
	Temperature	°C
	Depth – as pressure	cmH_2O
Water chemistry variables – field	Electrical Conductivity	µS cm^{-1}
	pH	units
	Temperature	°C
Water chemistry variables – laboratory	Ag, Al, As, Au, B, Ba, Be, Bi, Br, Cd, Ce, Co, Cr, Cs, Cu, Dy, Er, Eu, Fe, Ga, Gd, Hf, Hg, Ho, I, In, La, Li, Lu, Mn, Mo, Nb, Nd, Ni, Os, Pb, Pd, Pr, Rb, Re, Sb, Sc, Se, Sm, Sn, Sr, Ta, Tb, Te, Th, Ti, Tl, Tm, U, V, W, Y, Yb, Zn, Zr	µg L^{-1}
	Ca, Cl, Mg, K, Na, SO_4 (as S)	mg L^{-1}
	HCO_3^-, OH^-, CO_3^{2-}, Total Alkalinity	mg L^{-1}
	Electrical Conductivity	µS cm^{-1}
	pH	units
	Total Nitrogen, NO_2, NO_3, NH_3, PO_4, Total Phosphate	mg L^{-1}
	Total Organic Carbon (TOC) and Dissolved Organic Carbon (DOC)	mg L^{-1}

2.3 Biota

Groundwater fauna were sampled from all piezometer sites (Figure 4) in both July and August. Additional samples were collected in July from a selection of the intact old bores found in the central channel (Bores 1 and 2, Figure 4). Samples were collected by lowering a weighted 63 µm plankton net to the bottom of the piezometer and retrieving it six times following the guidance of the Western Australian Environmental Protection Authority (Environmental Protection Authority 2013). The contents of each haul were emptied into a 63 µm sieve and the total sample placed into a 60 mL Greiner tube and preserved with 100% absolute ethanol. The net was rinsed between sites to minimise contamination.

In the laboratory, fauna were removed from the samples by sorting under a low power dissecting microscope. Fauna were identified to the lowest taxonomic level possible using available keys.

One sample (MCMB02 from July 2016) was sorted using a Rose Bengal stain to aid in separation of specimens from the sediment/detritus of the samples. This was done because the sample contained significant amounts of sediment/detritus compared to the six that had already been sorted from the August 2016 collection.

---

[2]. Eaton AD, Clesceri LS, Rice EW & Greenberg, AE (eds) 2005. *Standard methods for the examination of water and wastewater.* American Public Health Association, American Water Works Association, Water Environment Federation, Washington, DC.

3 Results and Discussion

3.1 Water Chemistry

3.1.1 Continuous data

Continuous monitoring of groundwater EC in the creek was carried out until just after the early rains caused the creek to start flowing in September (Figure 8). The CTD-Divers were removed at this point as a number of the piezometers were damaged during the high flows. Upstream EC (MCMB01) tended to be relatively stable, with a median of 41 µS cm^{-1} until the creek flowed, when it dropped to 8 µS cm^{-1}, slowly increasing as flow and surface water levels dropped (Figure 8). The highest EC was measured at MCMB03, reaching a maximum of 566 µS cm^{-1} on the 19th of September. MCMB03 displayed some unusual EC peaks during the sampling period. Those seen in September are presumably associated with the large rainfall events preceding creek flow (Figure 9); however, the August EC peaks are less well explained. There were small localised rainfall events in August, that were captured by the rainfall records for G8210009 (009) and Djalkmara LAA monitoring stations (Figure 9), which appear to correspond to the EC peaks seen in the MCMB03 data. Alternatively, these peaks could indicate the passage of a localised pulse of contaminated water and/or differential pathways of contaminant flow through the subsurface sands over time. As with the remainder of the sites, once flow commenced, EC at MCMB03 dropped significantly (21 µS cm^{-1}). However, levels quickly rose once the surface water levels dropped (Figure 8). EC at MCMB06 increased significantly after early rains at the beginning of September (Figure 8). This site was situated at the outlet of CJBB and the results could indicate a preferential groundwater pathway flow out of CJBB. MCMB07 had small EC peaks with the September rainfall events and, once Magela Creek levels dropped, showed a marked increase in EC. These peaks may be associated with mobilisation of contaminants in groundwater sourced from historical LAAs. It was also noted that riparian vegetation adjacent to MCMB07 appeared degraded (Figure 10).

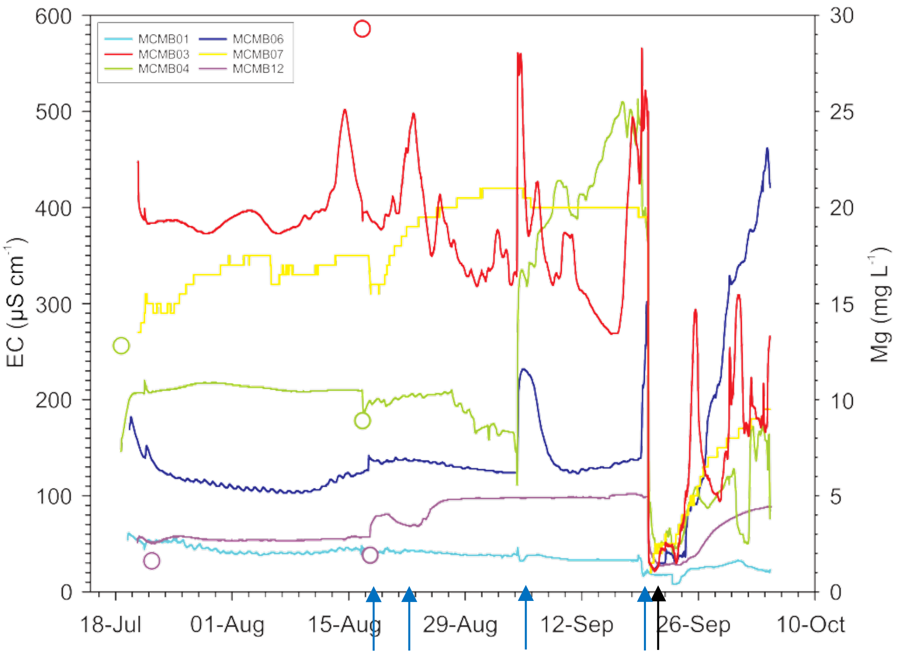

Figure 8 Continuous EC data measured with CTD divers from selected bores. Open circles are associated magnesium data for MCMB03 (red), MCMB04 (brown) and MCMB12 (purple). Rainfall events are indicated by blue arrows and September flow event is indicated by a black arrow.

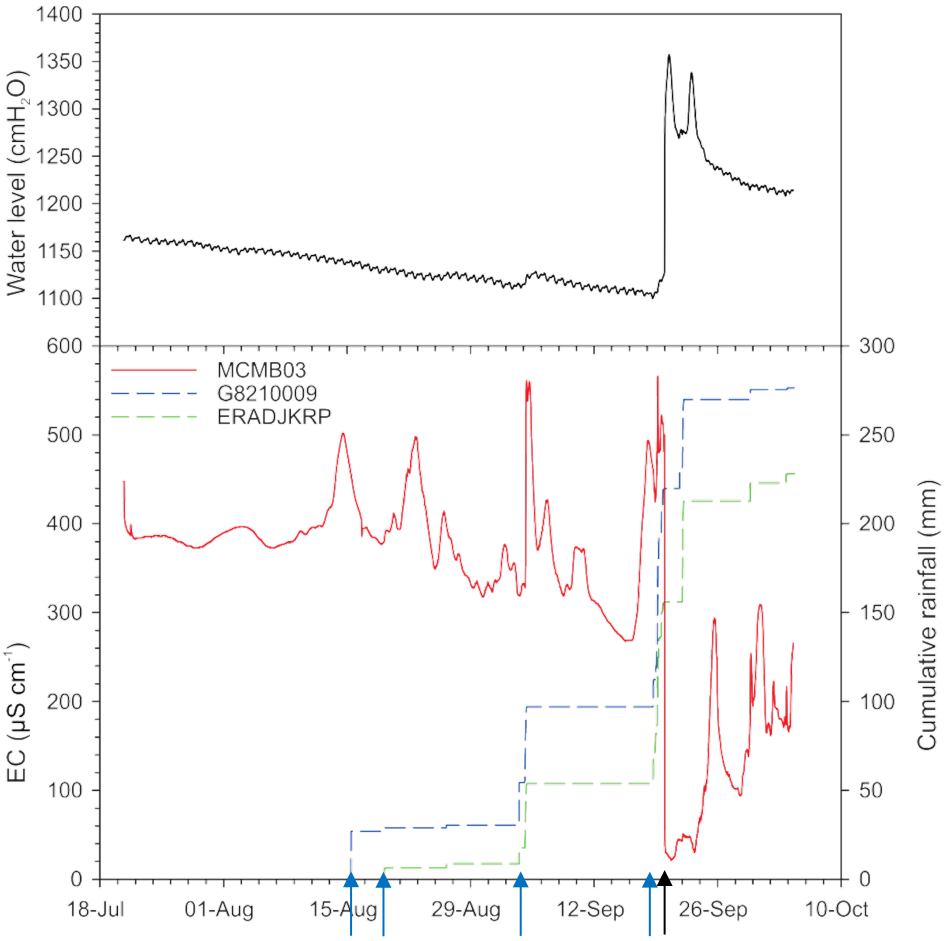

Figure 9 Continuous EC data measured at MCMB03. Dashed lines are cumulative rainfall data from 009 gauging station in Magela Creek (blue) and ERA's monitoring station in Djalkmara LAA (green). Top graph is water level in MCMB03 as measured by the CTD diver in cmH$_2$O. Rainfall events are indicted by blue arrows and September flow event is indicated by a black arrow.

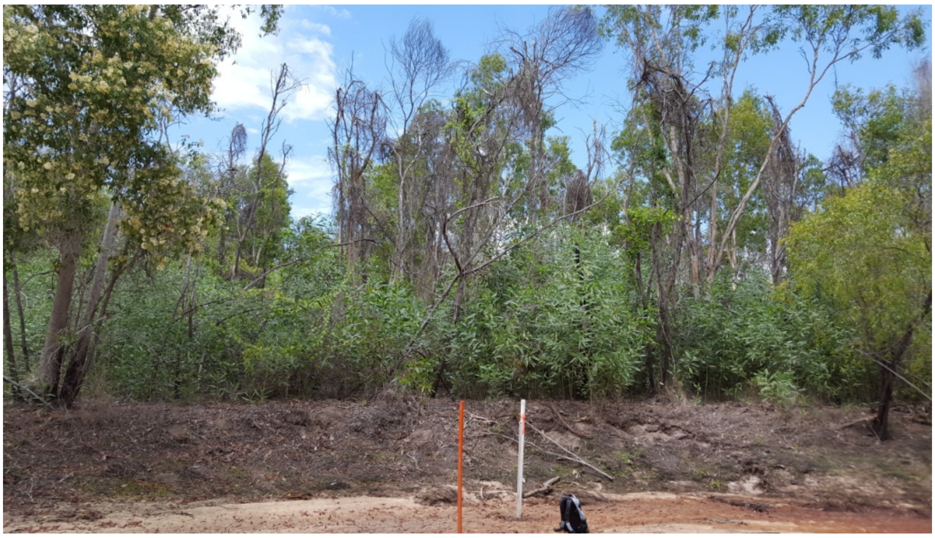

Figure 10 Riparian vegetation adjacent to MCMB07

3.1.2 Water quality determined from analysis of grab samples

Water quality data collected in July and August indicated the groundwater within Magela Creek sand channel is generally mildly acidic (Table 4), similar to the creek's surface waters (Table 5). MCMB01 and MCUS values in Tables 4 and 5 respectively reflect values uninfluenced by mining at Ranger. The deeper sample from MCMB04 had slightly lower pH (4.8) than all other sites (Table 4).

Table 4 Major contaminants of potential concern measured in July and August 2016. Surface (~1 m) and depth (~3.6 m) readings collected in July. Only 'surface' readings (see Table 2 for casing depths) were collected in August. Filtered ions and metals are highlighted here. All water chemistry data are summarised in Appendix 1.

Site	Field EC (µS cm^{-1})	Field pH	Lab EC (µS cm^{-1})	Lab pH	Mg (mg L^{-1})	S[1] (mg L^{-1})	U (µg L^{-1})	Mn (µg L^{-1})
July								
MCMB01 - surface	43.9	6.21	31	6.6	1.8	0.02	0.027	42.2
MCMB01 - depth	29.7	5.76	20	6.1	0.7	0.07	0.005	39.1
MCMB02 - surface	46.7	5.53	26	6.6	1.3	0.07	0.087	142
MCMB02 - depth	43.4	5.48	26	6.5	1.5	0.10	0.089	80.3
MCMB04 - surface	214.3	5.24	224	5.5	12.8	27.84	0.058	167
MCMB04 - depth	209.9	4.95	237	4.8	10.7	29.44	0.02	252
MCMB12 - surface	53.4	5.55	40	6.5	1.6	0.13	0.08	133
MCMB12 - depth	63.2	5.9	42	7	2.4	0.03	0.077	182
August								
MCMB01	52.7	5.85	39	6.1	1.8	0.13	0.026	77.4
MCMB02	56.5	6.17	38	6.4	2	0.03	0.076	313
MCMB03	372.2	5.56	370	6.1	29.3	45.73	0.062	452
MCMB04	201.5	5.12	182	5.6	8.9	18.49	0.065	87.1
MCMB06	116.1	5.85	124	6.3	7.8	5.01	0.11	58.9
MCMB07	308.5	5.28	272	5.4	16.5	35.71	0.039	272
MCMB12	53.4	6.39	35	6.5	1.9	0.13	0.034	91.3

[1] The use of total S measured by ICP-AES to infer SO_4 in water assumes that in oxic surface waters, of the type generally studied by SSB, the majority of the S will be present as SO_4. Any other S species, such as organic S, sulfide, sulfite, and thiosulfate, should be present in concentrations much lower than SO_4 due to the physicochemical conditions of the waters (Harford et al 2014). As groundwaters do not have the same oxic conditions we have recalculated S by dividing by the stoichiometric conversion factor of 2.996 (Reisman et al 2007)

Table 5 Surface water chemistry ranges for MCDW, MCUGT, and MCUS

Site	Field EC (µS cm^{-1})	Lab EC (µS cm^{-1})	Field pH	Mg (mg L^{-1})	SO_4 (mg L^{-1})	U (µg L^{-1})	Mn (µg L^{-1})
MCUS[a]	4.53-24	3.42-26	4.69-7.62	0.1-1.1	0.03-3.55	0.005-2.8958	0.95-41.48
MCUGT	2.2-22.5[b]	n/a	4.67-7.02[b]	0.1-1.1	0.1-6	0.006-0.064	0.21-17
MCDW	3.9-130.1[b]	n/a	4.68-7.53[b]	0.2-7.1	0.1-26.5	0.016-0.743	0.71-22

[a] MCUS data collated from ERA LIMS database (December 1993-current see (Illes 2003, 2004, Illes et al 2004) for rationale of not including pre 1993 data)

[b] Field EC and pH taken from SSB continuous monitoring station data (recorded from December 2005-current)

Higher than reference EC values were recorded from the sites around CJBB (MCMB03-MCMB07), reflecting the results observed in the continuous monitoring data. The elevated EC appears to be due primarily to elevated levels of Mg, Cl and SO_4 (Figure 11 and 12). High levels of

K (13.7 mg L^{-1} and 13.9 mg L^{-1}) were recorded at MCMB04 in July. However, these levels were not observed in the August samples (maximum of 1.5 mg L^{-1} at MCMB01, Figure 12).

The ionic composition of subsurface waters collected from selected sites in August 2017 is shown in Figure 13 as Schoeller diagrams (ie plots of relative concentrations (Y axis) of various anions and cations (X axis) from multiple samples on a single graph). The water quality of sites around CJBB show similar ionic composition to the billabong at the time of sampling and are different from the upstream reference site MCMB01 and downstream MCMB12 sites, indicating waters from the billabong are a possible source for the contamination.

The deep sample collected from MCMB04 in July had concentrations of total metals many (1-2) orders of magnitude higher than those collected from all other sites (Appendix 1; this is also discussed further in section 3.1.3).

Filtered samples of metals also showed some elevation in concentration at the 'exposed' sites compared to reference sites, particularly Mn, Ba and B (Figure 11 and 12). The exposed sites also had significantly higher values of S (Table 4, Figure 11 and 12), and a sulfurous odour was noted at MCMB03 and MCMB07 in August.

3.1.2.1 Caveats around water chemistry sampling

For this pilot study, dissolved oxygen and redox variables were not able to be measured reliably. Water chemistry results may be influenced by both of these variables.

Water chemistry samples can also be influenced by the concentrations of fine sediment material, particularly the results for total metals. The data reported here do not account for this.

These aspects will need to be addressed in any future sampling and the data reported here should be revisited in the context of any future information acquired.

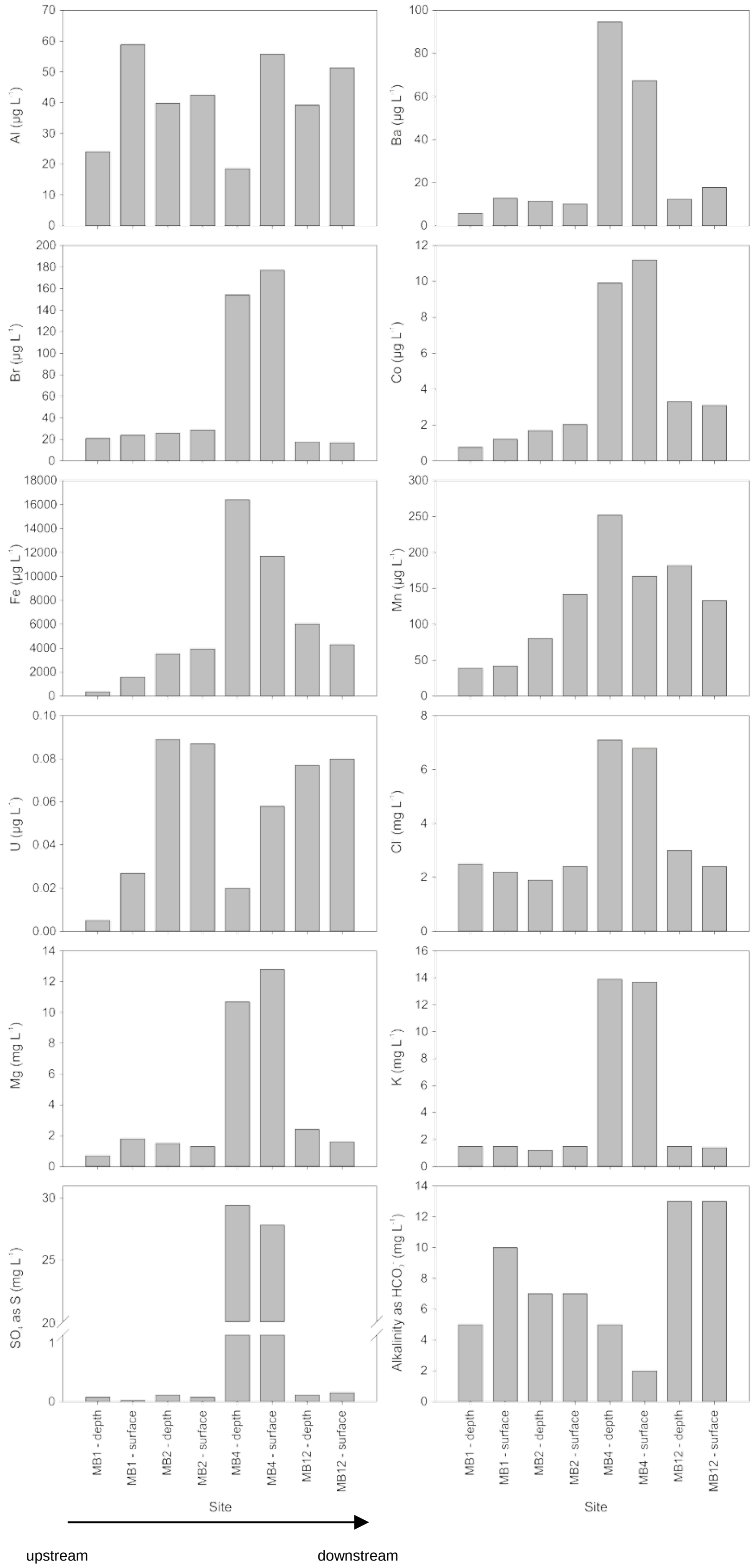

Figure 11 Filtered concentrations of analytes of potential interest. July sampling Sites are separated into surface and depth.

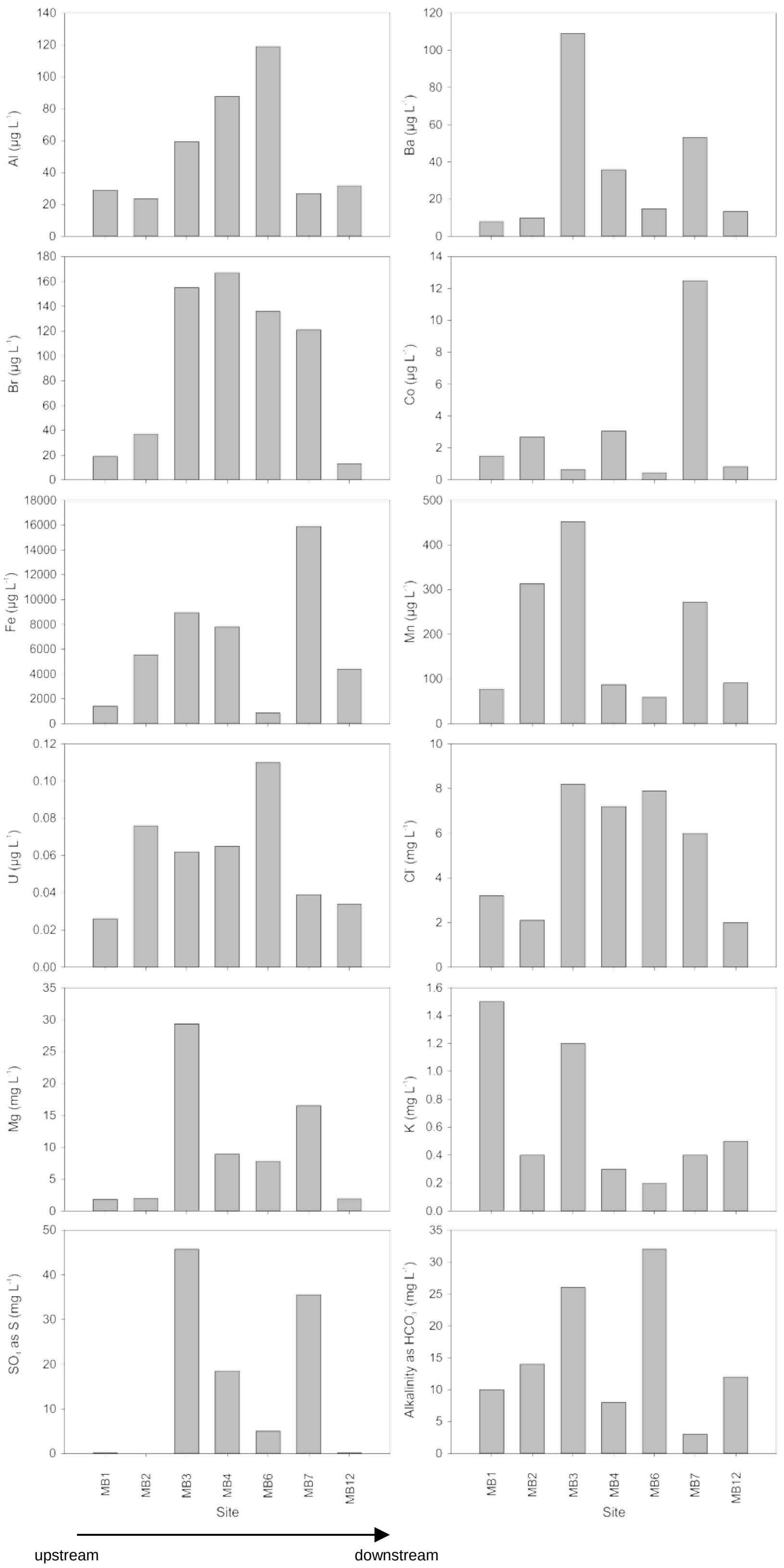

Figure 12 Filtered concentrations of analytes of potential interest. August sampling

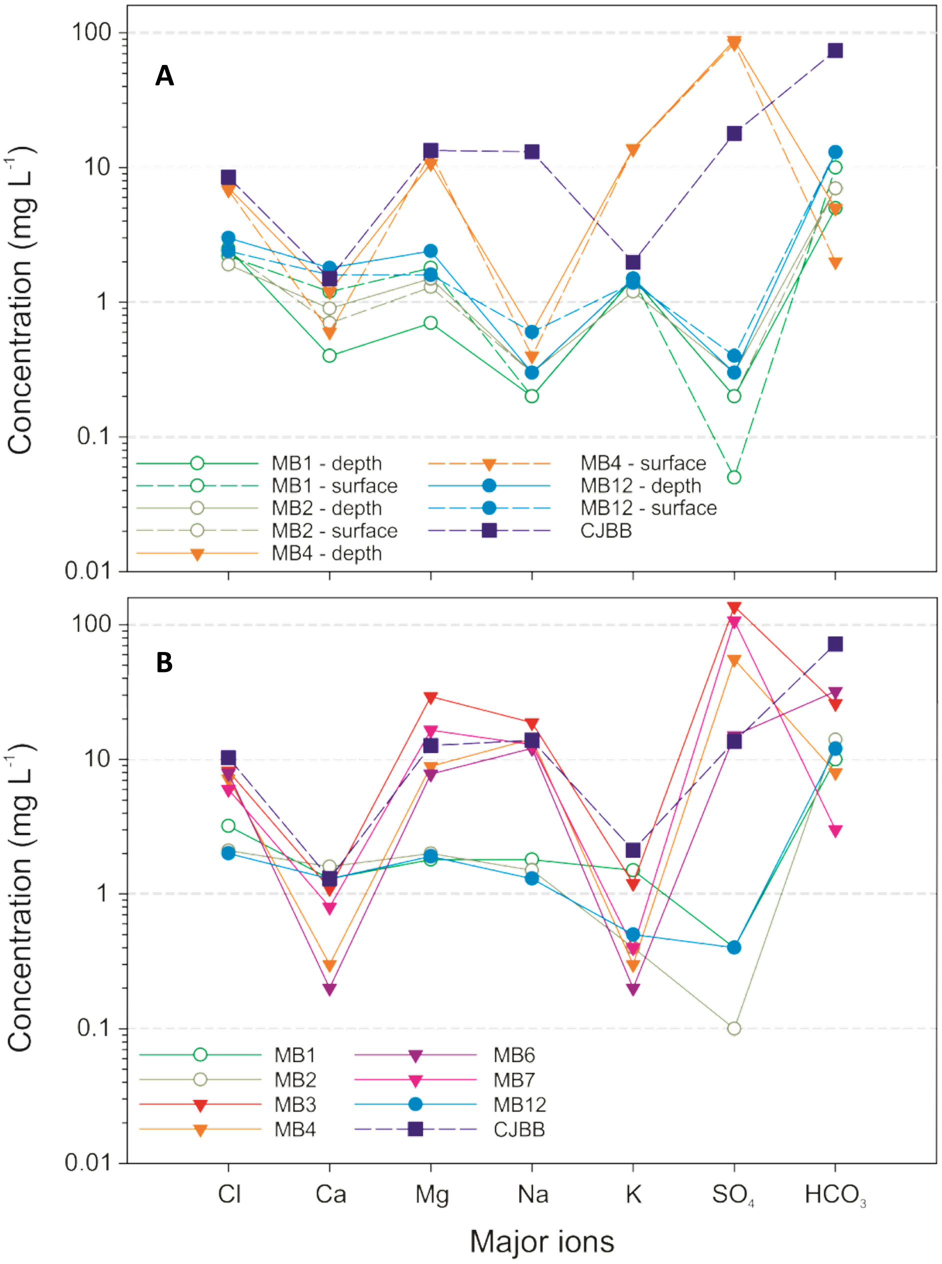

Figure 13 Schoeller diagrams for A) July and B) August 2016 sampling periods. Associated Coonjimba Billabong data (from ERA LIMS database) also plotted.

3.1.3 Principal Component Analysis – Water chemistry data

Principal Components Analysis (PCA) is an ordination in which samples (or points in high-dimensional variable space) are projected onto a best-fitting plane in two dimensional space, illustrating as much of the variability in the original high dimension space as possible (Clarke & Warwick 2001). It can be used to identify important gradients in environmental data. Complete results for the PCA conducted on water chemistry variables (both filtered and total concentrations) are described in Appendix 2. Figure 14 shows results for combined total and filtered concentrations while Figure 15 shows results for just filtered concentrations.

Results for Axes 1 and 2 of the PCA analysis for combined total and filtered concentrations, accounting for 67.4% of the total sample variance (41.2% and 26.2% respectively), are shown in Figure 14. The figure designates sampling locations according to site, exposure type and sampling depth.

Principal Component Axis 1 (PC1), accounting for 41.2% of the sample variance, is primarily influenced by total metal concentrations, which appears to be related to the depth at which the sample was collected. The deeper MCMB04 sample (collected from approximately 3.6 m depth in July 2016) had significantly higher concentrations of total metals than was recorded from all other sites. Increased concentrations of some of the rare earth elements (eg Er Eu, Gd Sm, Y) in the samples collected at 3.6 m (particularly from MCMB04) compared to all other samples are the primary contributors to the spread of samples along the PC1 axis (eg ln(Y_T) has coefficients -0.146 and -0.015, so its main contribution is to PC1, increasing from right to left because the coefficient is large and negative). Higher concentrations of CoPCs, such as U (39.9 µg L^{-1} compared to rest of the sites < 0.5 µg L^{-1} on average), were also recorded from the MCMB04 deep sample and contribute to the distribution of sites along the PC1 axis (Figure 14a). The elevated levels of total metals in this sample could be related to high amounts of fine suspended sediments in the sample, for example high Al can be associated with the occurrence of suspended clays. However this result needs to be examined further as only one sample was collected from the exposed sites at depth.

Principal Component Axis 2 (PC2), accounting for 26.2% of the sample variance, best separates exposed sites near CJBB from sites in essentially reference condition, ie upstream, well-downstream and central channel. PC2 depicts a water quality gradient (from right to left) associated with the mine derived contaminant Mg (Figure 14b) and filtered metals (predominantly the rare earth elements, eg Er).

Considering the possible influence of fine suspended sediments on the results of the total metals analysis and corresponding PCA (Figure 14), an additional PCA was also performed examining the filtered results only. Complete results for this PCA can be found in Appendix 2 (Tables A2.3 and A2.4). Results for Axes 1 and 2 of the follow-up PCA, accounting for 57.8% of the total sample variance (43% and 14.8% respectively), are shown in Figure 15. The figure designates sampling locations according to site, exposure type and sampling depth.

PC1, accounting for 43% of the separation between sites, is primarily influenced by S (Figure 15b) and Mg. As for PC2 in the combined PCA (Figure 14), this Axis best separates the exposed sites near CJBB from sites in essentially reference condition depicting a water quality gradient associated with increasing concentrations of Mg and S (from right to left, Figure 15).

PC2, accounting for 14.8% of the separation between sites, is influenced by a number of different variables (see Table A2.4 in Appendix 2). The primary contributors to the distribution along PC2 are Al and Ce, with Ni, K and HCO_3 also exerting influence.

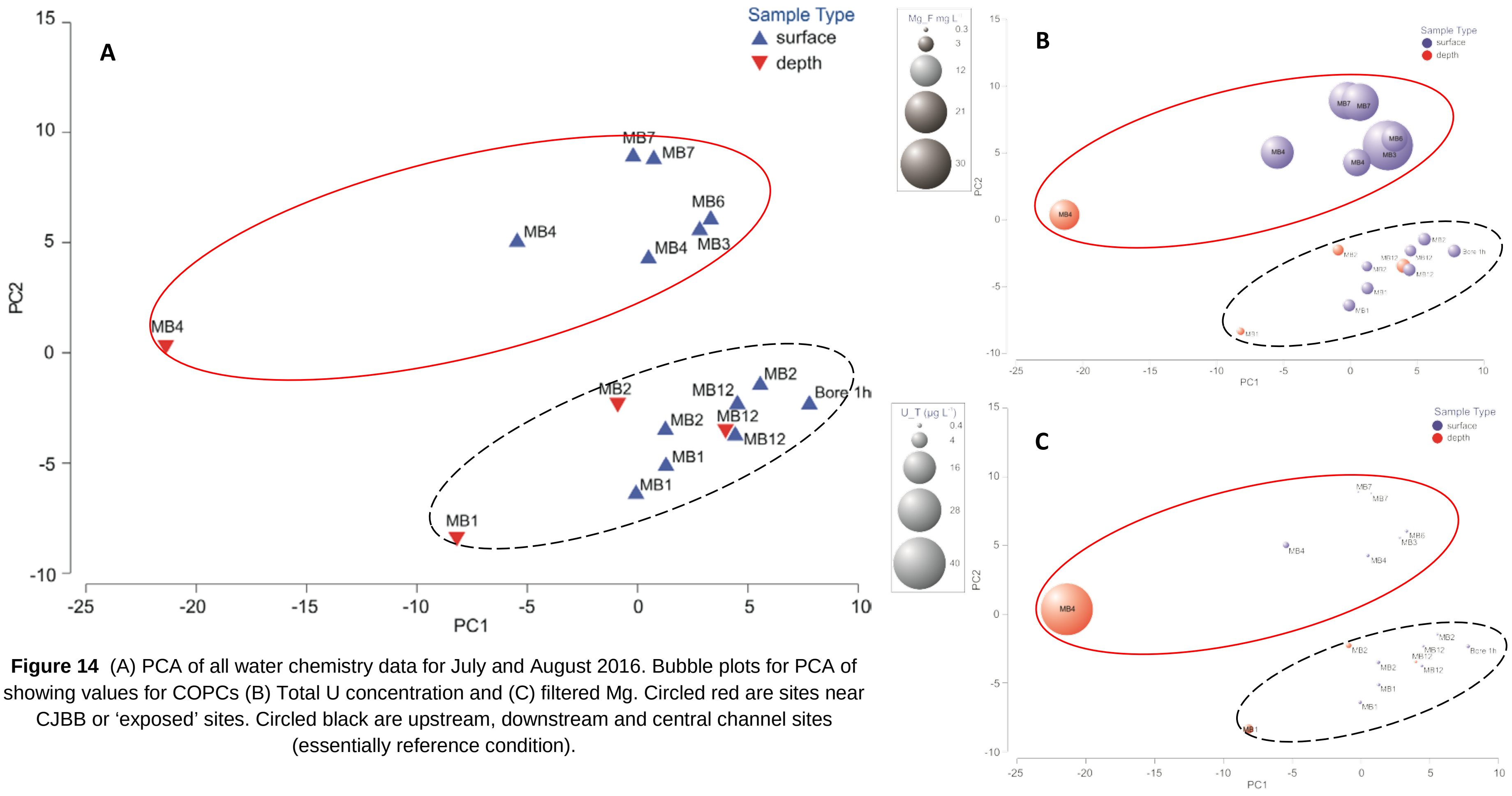

Figure 14 (A) PCA of all water chemistry data for July and August 2016. Bubble plots for PCA of showing values for COPCs (B) Total U concentration and (C) filtered Mg. Circled red are sites near CJBB or ‘exposed’ sites. Circled black are upstream, downstream and central channel sites (essentially reference condition).

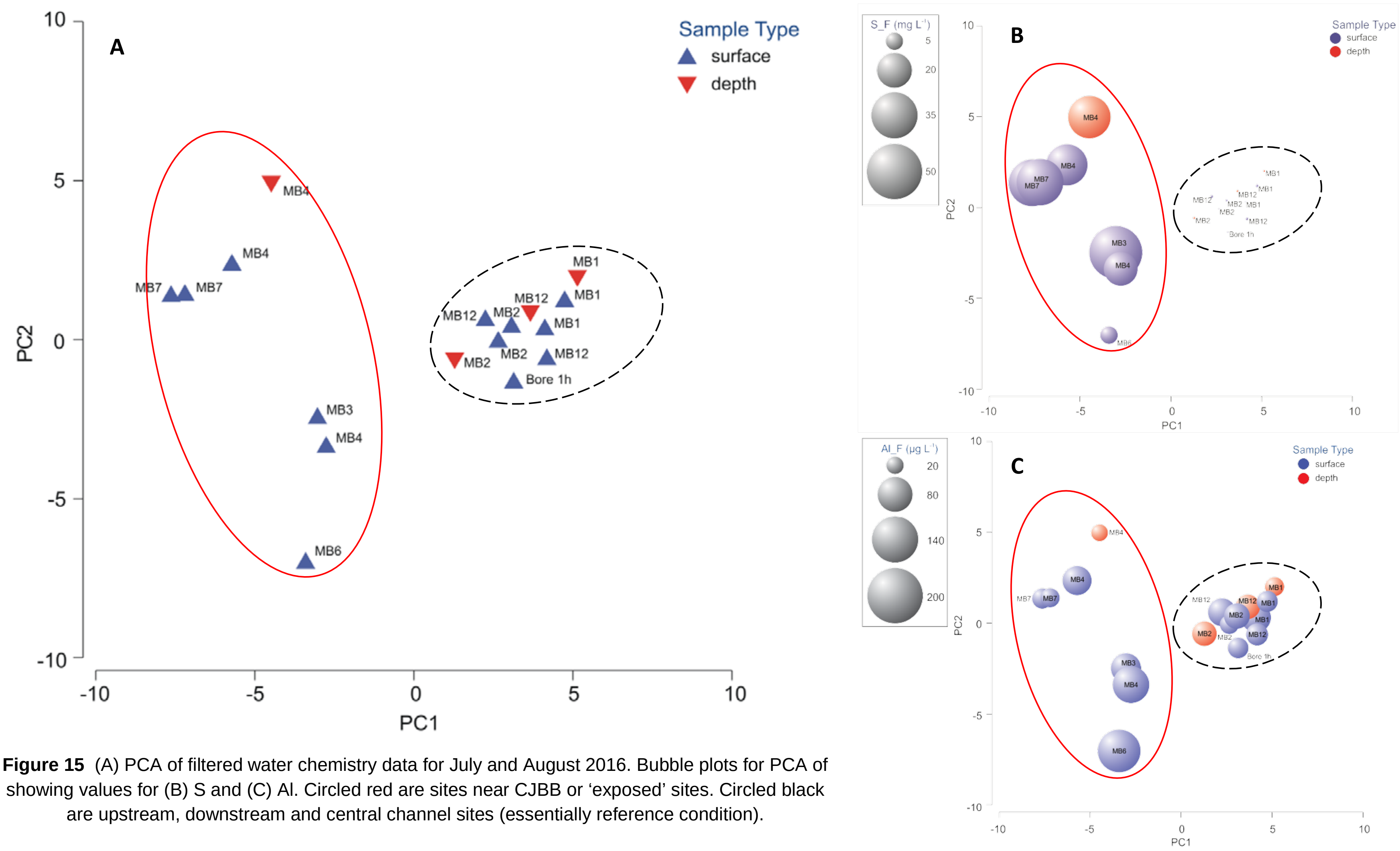

Figure 15 (A) PCA of filtered water chemistry data for July and August 2016. Bubble plots for PCA of showing values for (B) S and (C) Al. Circled red are sites near CJBB or 'exposed' sites. Circled black are upstream, downstream and central channel sites (essentially reference condition).

3.1.5 Source and transport of subsurface contamination in Magela sand channel

The variation in EC amongst sites analysed for this pilot study is consistent with a source of contaminated mine waters arising in the vicinity of CJBB. EC was highest at MCMB03, immediately adjacent to CJBB, but declined with progressive distance downstream, while EC at sites upstream of MCMB03 were amongst the lowest recorded (Table 4).

From December 2015 sampling it was hypothesised (Section 1.3) that subsurface contamination of the Magela sand channel would travel in a pulse downstream over the duration of the dry season, given that flow in the subsurface sands occurs for the duration of the dry season (Ahmad et al 1982). The premise for this model of transport is that the primary input of contamination occurs during the wet to wet-dry transition period. If this was the case, then sites near the CJBB confluence might be expected to decline in EC while those downstream of CJBB would progressively increase in EC over the dry season. The pulses observed in the 2016 dry season data appear to be associated with localised rainfall events (Figures 8 and 9). These events appear to have mobilised solutes at sites 3, 4, 6 and 7, given the sharp pulse or increase in EC observed at these sites at that time (Figure 8). The unusually early rainfall events and subsequent flow in September 2016 thwarted any ability to effectively test the hypothesis of a moving pulse through the dry season of contaminated subsurface waters downstream from a source near CJBB.

3.2 Biota

Eight samples had been examined by the conclusion of this study. Results are shown in Table 6.

Excluding taxa of terrestrial origin (ie Collembola and Pauropoda) a total of 144 individuals from 13 taxa were collected. Nematodes, oligochaete worms and harpacticoid copepods were the most abundant taxa (Table 6).

The majority of the specimens collected cannot be confidently identified as obligate groundwater fauna due to the presence of convergent morphological characteristics in subsurface taxa (Gibert et al 1994). Species-level identification will require assistance from taxonomic experts and potentially DNA-sequencing.

A number of specimens of Syncarida (Figure 16) were collected from MCMB02. These specimens were tentatively identified as members of the family Parabathynellidae. Syncarida are small crustaceans that primarily inhabit interstitial groundwater (Camacho & Valdecasas 2008). Australian parabathynellids have been found to be quite diverse with restricted distributions (Abrams et al 2013, Cho 2005, Cho et al 2006) and so have conservation significance.

The parabathynellid specimens collected from Magela Creek are potentially a new record for the Northern Territory. Currently only one species (*Atopobathynella readi*) has been recorded from the Northern Territory (Cho et al 2006), collected from bores on Newhaven Station (approximately 300 km NW of Alice Springs) and, given the restricted nature of known species distributions, it is likely the Magela specimens represent a new species.

Harpacticoid copepods were collected in relatively high numbers from MCMB02. Harpacticoids have been shown to be sensitive to environmental variables, including metals (Burton et al 2002, Di Marzio et al 2009, Hose et al 2016).

The variability apparent in the biotic data is characteristic of results from surveys of groundwater fauna (eg Galassi 2001). At the microspatial scale groundwater fauna show marked differences in microhabitat preferences (Galassi et al 2009), and groundwater taxa separated by even several hundred metres may show strong genetic divergence (Hose et al 2016)

These results must be regarded as a preliminary assessment, as a total of 40 samples taken from at least 10 bores are required for adequate conservation assessment (Environmental Protection Authority 2013). Tang and Eberhard (2016) highlight, even with intensive biannual field sampling and specimen identification efforts over 15 years, new species continue to be detected from sites that had been sampled many times previously. Absence of taxa from a sample is not definitive evidence of absence from that habitat (Environmental Protection Authority 2013, Hose & Lategan 2012), so it can be assumed that the composition of the subsurface community is likely to be greater than indicated by these results. Nevertheless, the results establish the presence of a groundwater community in the subsurface of the Magela Creek sand channel.

Table 6 Taxa collected in samples from July and August 2016. Sty = stygofauna, T = terrestrial or troglofauna, S = surface water, U = unclassified due to lack of taxonomic discrimination at this point.

		MCMB01	MCMB02	MCMB02	MCMB04	MCMB05	MCMB11	MCMB12	B1H
Taxon	***Source of fauna***	16/08/2016	21/07/2016	16/08/2016	16/08/2016	16/08/2016	17/08/2016	17/08/2016	21/07/2016
PLATYHELMINTHES									
Turbellaria spp.	U		1						
NEMATODA									
Nematoda spp.	U	1	5		1		20		
ANNELIDA									
Oligochaeta spp.	U	5	4		4		9	7	
CRUSTACEA									
CLADOCERA									
Cladocera spp.	U		1						6
COPEPODA									
Cyclopoida spp. (imm.)	U			2					1
Cyclopoida spp.	U		1						1
Harpacticoida spp.	Sty?		42						
SYNCARIDA									
?Parabathynellidae spp.	Sty		15	1					
ARACHNIDA									
ORIBATIDA									
Oribatida spp.	U	2		2					
PROSTIGMATA									
Acarina spp.	U	2	1						
MYRIAPODA									
PAUROPODA									
Pauropoda spp.	T				1		3		
COLLEMBOLA									
Collembola sp1	T							1	

		MCMB01	MCMB02	MCMB02	MCMB04	MCMB05	MCMB11	MCMB12	B1H
Taxon	***Source of fauna***	16/08/2016	21/07/2016	16/08/2016	16/08/2016	16/08/2016	17/08/2016	17/08/2016	21/07/2016
Collembolla sp2	T					1			
INSECTA									
unknown Coleopteran larvae	T				1				
unknown imm Insecta	U	1							
Chironomidae spp. (L)	S		5						
Tabanidae spp. (L)	S		2	2					
Total number of taxa		***5***	***9***	***4***	***4***	***1***	***3***	***2***	***3***
Total Abundance		***11***	***76***	***7***	***7***	***1***	***32***	***8***	***8***

Figure 16 Syncarid specimens collected from MCMB02 in (A) July, pink colour due to use of Rose Bengal stain in the sorting process, and (B) August.

4 Conclusions and future work

4.1 Water Chemistry

There is little baseline water quality data for subsurface waters in the Magela Creek sand channel. Water quality in piezometers upstream of Ranger displayed similar characteristics to the natural Magela Creek surface waters (ie low conductivity, alkalinity and concentrations of major ions). Water chemistry data have indicated there is mine-associated contamination (eg increased concentrations of Mg and other CoPCs) occurring in the western channel of Magela Creek adjacent to CJBB, this is supported by:

1. Sites adjacent to CJBB (MCMB03-MCMB07) show similar ionic composition to CJBB and other mine impacted sites (RP1 and Jabiru East LAA see (Baldwin 2017).
2. CJBB has experienced a decline in water quality since the early 1980s. The artificial waterbody, Retention Pond 1 was constructed in the upper Coonjimba Creek catchment and directly affects the water quality of CJBB through passive and/or active release of mine waters during the wet season resulting in increased concentrations of $MgSO_4$ and other CoPCs (see (Humphrey & Chandler 2017)) and development of potential acid sulfate sediments (Baldwin 2017).
3. CJBB is also aligned with a potential contaminant pathway from the Tailings Storage Facility (URS 2010), which may be expressing through shallow groundwater.
4. Water quality at piezometers installed downstream of the CJBB area and within the adjacent c central channel is similar to that from upstream reference sites.

Further sampling is required to determine the source, rate of movement and extent of this contamination – longitudinally, latitudinally, through the sands depth profile and over time. To achieve this, the following additional sites in Magela Creek are recommended:

1. Installation of piezometers between ERA's MG005 station and the MCMB03 site to determine whether contamination extends further upstream, and to establish a baseline prior to the predicted solute egress following closure.
2. Installation of piezometers on the eastern side of the western channel near MCMB03 to determine whether the contamination extends across the creek channel.
3. Installation of deeper piezometers to determine whether contamination extends through the depth profile.

To assist with development of baseline data, the following additional sites are recommended:

1. Installation of at least one piezometer further downstream of MCMB02 site, near the confluence of Djalkmara Creek (Indium Billabong), to examine potential movement of contaminants associated with Pit 3 via the Djalkmara Creek.
2. Installation of piezometers near the Georgetown Billabong confluence to examine potential movement of contaminants associated with Pit 1 via Corridor Creek, or from the Magela Land Application Area.
3. Installation of at least one piezometer further upstream from MCUS to ensure there is no influence from Ranger mine Project Area.

Further depth profiles are critical to characterising natural gradients in water quality through the sand profile, as well as the contamination around Coonjimba Billabong and elsewhere. Access to the deeper sands (>3.6 m) is not possible using the current equipment.

Redox and dissolved oxygen were not measured due to instrument limitations (section 3.1.2.1). This will need to be redressed in any future sampling to assist in the interpretation of biological and water chemistry data.

Any long-term sampling within the creek channel needs to consider surface flow and the stability of the installed infrastructure. A number of the piezometers installed for this pilot were broken during the initial flush of surface flow that occurred in September. Installing these so there is less of the PVC pipe remaining above the sand surface, ie installation of the slotted section slightly deeper and installing a second pipe around the outside of the piezometer, could help protect against debris and surface flow. More robust stainless steel piezometers may also be deployed.

4.2 Biota

Despite the limited number of samples and of sampling occasions, the study has proven the presence of aquatic fauna in the deeper sands of Magela Creek (> ~0.3 m). Diversity and abundance are apparently low but greater temporal replication of sampling is needed to determine if this is a seasonal phenomenon. Sampling of groundwater fauna in bores in the ancestral Magela sands (ie within Djalkmara LAA Figure 4) would provide information on the extent and composition of the stygofauna community and its resilience to poor water quality due to solute egress from the rehabilitated site.

Groundwater across the Ranger mine site is conceptualised as occurring in two flow systems, an upper unconfined flow system restricted to alluvium and weathered rock and draining towards Magela Creek, and a deep slowly moving flow system within fractured bedrock with an overall northwards flow (GeoSciences Australia 2014). Further water chemistry and biotic sampling would assist in confirming and refining this conceptual model and providing a baseline for future monitoring of the impacts of surface and groundwater solute egress from the mine site.

4.3 Future work

- Complete sorting of remaining biotic samples.
- Revisit samples collected by Paltridge et al (1997), where they are still intact.
- Further biotic sampling, including genomic work.
- More detailed water chemistry analysis to extend temporal replication, including measurement of dissolved oxygen and redox.
- More depth profiles (only one sampling period of this, and this was only at one site around the CJBB contamination point).
- Construction of deeper bores to investigate the extent of contamination beyond the 3.6 m limit of our current sampling equipment.
- Expand the sampling to other streams;
    - GCT2 where there is an existing contamination
    - Gulungul Creek, and
    - Nourlangie and Burdulba Creeks as reference sites and to determine a spatial scale of groundwater fauna in alluvial sediments in ARR.
- Investigate the sources of contamination. Potential sources are Coonjimba Billabong and/or the Djalkmara LAA.
- Improve understanding of the behaviour of the solute contamination following dilution during flow events in the wet season, in light of the observed rapid elevation of EC levels observed during the pilot project.
- Determine the sensitivity of biota to contaminants of potential concern, using both existing contaminant gradients and laboratory testing of whole organisms and/or genomic characterisation of exposed substrates.

References

Abrams KM, King RA, Guzik MT, Cooper SJB & Austin AD 2013. Molecular phylogenetic, morphological and biogeographic evidence for a new genus of parabathynellid crustaceans (Syncarida : Bathynellacea) from groundwater in an ancient southern Australian landscape. *Invertebrate Systematics* 27 (2), 146-172.

Ahmad M & Salas G 1981. Regional hydrogeology of the Ranger area. Department of Transport and Works, Darwin. Technical Report WRD81035.

Ahmad M, Salas G & Scott F 1982. Stream bed underflow studies in the Magela Creek. Northern Territory Geological Survey Technical Report, Department of Mines and Energy, Darwin.

Baldwin DS 2017. Understanding acid sulfate soils in Coonjimba Billabong. Prepared for the Supervising Scientist Branch, the Department of Environment and Energy by Rivers and Wetlands. Final Report.

Boulton AJ, Findlay S, Marmonier P, Stanley EH & Valett HM 1998. The functional signficance of the hyporheic zone in streams and rivers. *Annual Review of Ecology and Systematics* 29, 59-81.

Bruce AJ 1992. *Pycnisia raptor*, a new genus and species of predatory troglobic shrimp (Crustacea : Decapoda : Atyidae) from northern Australia. *Invertebrate Taxonomy* 6 (3), 553-566.

Burton SM, Rundle SD & Jones MB 2002. Evaluation of the meiobenthic copepod *Bryocamptus zschokkei* (Schmeil) as an ecologically-relevant test organism for lotic freshwaters. *Journal of Aquatic Ecosystem Stress and Recovery* 9 (3), 185-191.

Camacho AI & Valdecasas AG 2008. Global diversity of syncarids (Syncarida; Crustacea) in freshwater. *Hydrobiologia* 595 (1), 257-266.

Cho J-L 2005. A primitive representative of the Parabathynellidae (Bathynellacea, Syncarida) from the Yilgarn Craton of Western Australia. *Journal of Natural History* 39 (39), 3423-3433.

Cho J-L, Humphreys WF & Lee S-D 2006. Phylogenetic relationships within the genus *Atopobathynella* Schminke (Bathynellacea: Parabathynellidae). *Invertebrate Systematics* 20 (1), 9-41.

Clarke KR & Warwick RM 2001. *Change in marine communities: an approach to statistical analysis and interpretation.* 2nd edition edn, Primer-E Ltd, Plymouth.

Di Marzio WD, Castaldo D, Pantani C, Di Cioccio A, Di Lorenzo T, Sáenz ME & Galassi DMP 2009. Relative sensitivity of hyporheic copepods to chemicals. *Bulletin of Environmental Contamination and Toxicology* 82 (4), 488-491.

Dumont HJ & Maas S 1985. *Mesocyclops cuttacuttae* n.sp. from a cave in Northern Australia (Crustacea: Copepoda: Cyclopoida). *Beagle: Records of the Museums and ARt Galleries of the Northern Territory* 1 (13), 115-122.

Eberhard SM, Halse SA & Humphreys WF 2005. Stygofauna in the Pilbara region, north-west Western Australia: a review. *Journal of the Royal Society of Western Australia* 88 (4), 167-176.

Environmental Protection Authority 2013. Environmental Assessment Guideline 12: Consideration of subterranean fauna in environmental impact assessment in Western Australia. Environmental Protection Authority, Perth.

ERA 2014. Ranger 3 Deeps Draft Environmental Impact Statement. Appendix 9. Solute Egress Modelling for ERA Ranger 3 Deeps mine closure. Energy Resources of Australia, Jabiru, NT, Australia.

Galassi DMP, Huys R & Reid JW 2009. Diversity, ecology and evolution of groundwater copepods. *Freshwater Biology* 54, 691-708.

Gibert J, Danielopol DL & Stanford JA (eds) 1994. *Groundwater Ecology.* Academic Press, San Diego.

Harford AJ, Hogan AC, Jones DR & van Dam RA 2014. Ecotoxicology of highly treated mine waters: lessons from an Australian mine. *Mine Water and the Environment* 34 (1), 75-86.

Hose GC & Lategan MJ 2012. Sampling strategies for biological assessment of groundwater ecosystems. CRC CARE Technical Report no. 21, CRC for Contamination Assessment and Remediation of the Environment, Adelaide, Australia.

Hose GC, Sreekanth J, Barron O & Pollino C 2015. Stygofauna in Australian groundwater systems: extent of knowledge. CSIRO, Australia.

Hose GC, Symington K, Lott MJ & Lategan MJ 2016. The toxicity of arsenic(III), chromium(VI) and zinc to groundwater copepods. *Environmental Science and Pollution Research* 23 (18), 18704-18713.

Humphrey CL & Chandler L 2017. *Use of field-effects information to inform surface water guideline values for magnesium sulfate in Magela Creek.* Supervising Scientist Report 212, Supervising Scientist, Darwin.

Illes M 2003. Review of water quality triggers, November 2003 progress report. Internal Report 463, Supervising Scientist Division, Canberra.

Illes M 2004. Water quality objectives for Magela Creek - revised November 2004. Internal Report 489, Supervising Scientist Division, Canberra.

Illes M, Camilleri CM & Pilley R 2004. Identification of key water quality data for Ranger uranium mine. Internal Report 442, Supervising Scientist Division, Canberra.

Jansen JD & Nanson GC 2004. Anabranching and maximum flow efficiency in Magela Creek, northern Australia. *Water Resources Research* 40 (4), W04503.

Leaney FW & Puhalovich AA 2006. Use of environmental tracers to better understand groundwater recharge/discharge processes, Ranger uranium mine, NT. CSIRO.

Moulds T & Bannick P 2012. Preliminary notes on the cavernicolous arthropod fauna of Judbarra/Gregory karst area, northern Australia. *Helictite* 41, 75-85.

Nanson GC, East TJ & Roberts RG 1993. Quaternary stratigraphy, geochronology and evolution of the Magela Creek catchment in the monsoon tropics of northern Australia. *Sedimentary Geology* 83, 277-302.

Noller BN 1991. Non-radiological contaminants from uranium mining and milling at Ranger, Jabiru, Northern Territory, Australia. *Environmental Monitoring and Assessment* 19 (1-3), 383-400.

Paltridge RM, Dostine PL, Humphrey CL & Boulton AJ 1997. Macroinvertebrate recolonization after re-wetting of a tropical seasonally-flowing stream (Magela Creek, Northern Territory, Australia). *Marine and Freshwater Research* 48 (7), 633-645.

Pettit NE, Bayliss P, Davies PM, Hamilton SK, Warfe DM, Bunn SE & Douglas MM 2011. Seasonal contrasts in carbon resources and ecological processes on a tropical floodplain. *Freshwater Biology* 56, 1047-1064.

Pidgeon RWJ & Boyden J 1993. Investigation of effects of seepage from Ranger land application area on fish in residual pools in Magela Creek.

Reisman DJ, Sundaram V, Al-Abed SR & Allen D 2007. Statistical validation of sulfate quantification methods used for analysis of acid mine drainage. *Talanta* 71, 303-311.

Roberts RG 1991. Sediment budgets and quaternary history of the Magela Creek catchment, tropical northern Australia. PhD Thesis, University of Wollongong, Department of Geography.

Sundaram B, Feitz AJ, de Caritat P, Plazinska A, Brodie RS, Coram J & Ransley T 2009. Groundwater Sampling and Analysis – A Field Guide. Geoscience Australia. Record 2009/27.

Supervising Scientist 2015. Annual Report 2014-15. Commonwealth of Australia.

Supervising Scientist 2017. *Alligator Rivers Region Technical Committee: Key Knowledge Needs: Uranium Mining in the Alligator Rivers Region.* Supervising Scientist Report 213, Supervising Scientist, Darwin, NT.

Supervising Scientist for the Alligator Rivers Region 1994. Supervising Scientist for the Alligator Rivers Region: Annual Report 1993-1994. Canberra.

Tang D & Eberhard SM 2016. Two new species of *Nitocrella* (Crustacea, Copepoda, Harpacticoida) from groundwaters of northwestern Australia expand the geographic range of the genus in a global hotspot of subterranean biodiversity. *Subterranean Biology* 20, 51-76.

Tomlinson M & Boulton AJ 2010. Ecology and management of subsurface groundwater dependent ecosystems in Australia - a review. *Marine and Freshwater Research* 61, (949), 936.

URS 2010. Independent hydrogeological review of the tailing storage facility at the Ranger uranium mine. Final report by URS Australia Pty Ltd to Energy Resources of Australia Ltd, Darwin.

Warfe DM, Pettit NE, Davies PM, Pusey BJ, Hamilton SK, Kennard MJ, Townsend SA, Bayliss P, Ward DP, Douglas MM, Burford MA, Finn M, Bunn SE & Halliday IA 2011. The 'wet–dry' in the wet–dry tropics drives river ecosystem structure and processes in northern Australia. *Freshwater Biology* 56, 2169-2195.

Williams WD 1964. Subterranean freshwater prawns (Crustacea: Decapoda: Atyidae) in Australia. *Australian Journal of Marine and Freshwater Research* 15 (1), 93-106.

Appendix 1 – Water chemistry data

Table A1.1 July 2016 water chemistry data. Blank cells indicate variable was not recorded for that site

Variable	**Unit**	**Site**								
		MB1	**MB1**	**MB2**	**MB2**	**MB4**	**MB4**	**Bore 1h**	**MB12**	**MB12**
		surface	**depth**	**surface**	**depth**	**surface**	**depth**		**surface**	**depth**
		19-Jul	**19-Jul**	**19-Jul**	**19-Jul**	**18-Jul**	**18-Jul**	**21-Jul**	**22-Jul**	**22-Jul**
Field EC	µS cm^{-1}	43.9	29.7	46.7	43.4			51.4	53.4	63.2
Field pH	units	6.21	5.76	5.53	5.48			5.88	5.55	5.9
Field Temperature	ºC	26.41	28.96	29.52	30.3			29.94	24.19	28.17
Filtered Metals										
Ag_F	µg L^{-1}	<0.05	<0.05	<0.05	<0.05	<0.05	<0.05	<0.05	<0.05	<0.05
Al_F	µg L^{-1}	58.9	24.1	42.5	39.8	55.8	18.6	28.1	51.3	39.2
As_F	µg L^{-1}	0.15	0.1	0.35	0.35	0.2	0.75	0.1	0.15	0.45
Au_F	µg L^{-1}	<0.01	<0.01	<0.01	<0.01	<0.01	<0.01	<0.01	<0.01	<0.01
B_F	µg L^{-1}	9	11.5	10	10.5	22	27.5	11	11	11.5
Ba_F	µg L^{-1}	12.8	5.94	10.2	11.6	67.4	94.6	8.26	17.8	12.4
Be_F	µg L^{-1}	<0.05	<0.05	<0.05	<0.05	0.15	0.2	<0.05	<0.05	<0.05
Bi_F	µg L^{-1}	<0.01	<0.01	<0.01	<0.01	<0.01	<0.01	<0.01	<0.01	<0.01
Br_F	µg L^{-1}	24	21	29	26	177	154	15	17	18
Cd_F	µg L^{-1}	0.02	<0.02	<0.02	<0.02	<0.02	<0.02	<0.02	<0.02	<0.02
Ce_F	µg L^{-1}	0.27	0.16	0.33	0.58	0.95	0.7	0.2	0.35	0.23
Co_F	µg L^{-1}	1.21	0.76	2.03	1.7	11.2	9.91	0.07	3.1	3.3
Cr_F	µg L^{-1}	0.4	0.7	0.5	0.4	0.4	0.3	0.1	0.7	1.1
Cs_F	µg L^{-1}	0.01	0.02	0.03	0.02	0.03	0.06	0.04	0.06	0.04
Cu_F	µg L^{-1}	0.18	0.42	0.25	0.23	0.13	0.61	0.05	0.15	0.13
Dy_F	µg L^{-1}	0.02	<0.01	0.02	0.03	0.06	0.04	0.02	0.03	0.02
Er_F	µg L^{-1}	<0.01	<0.01	0.01	0.02	0.03	0.02	0.01	0.01	<0.01
Eu_F	µg L^{-1}	<0.01	<0.01	<0.01	0.01	0.02	0.01	<0.01	<0.01	<0.01
Fe_F	µg L^{-1}	1600	382	3950	3550	11700	16400	1650	4300	6050
Ga_F	µg L^{-1}	0.01	<0.01	0.02	0.01	<0.01	<0.01	<0.01	<0.01	0.02
Gd_F	µg L^{-1}	0.03	0.02	0.03	0.06	0.09	0.07	0.03	0.04	0.02
Hf_F	µg L^{-1}	0.01	<0.01	0.01	0.01	<0.01	<0.01	<0.01	<0.01	<0.01
Hg_F	µg L^{-1}	<0.02	<0.02	<0.02	<0.02	<0.02	<0.02	<0.02	<0.02	<0.02
Ho_F	µg L^{-1}	<0.01	<0.01	<0.01	<0.01	0.01	<0.01	<0.01	<0.01	<0.01
I_F	µg L^{-1}	<5	<5	5	5	30	40	<5	<5	<5
In_F	µg L^{-1}	<0.01	<0.01	<0.01	<0.01	<0.01	<0.01	<0.01	<0.01	<0.01
La_F	µg L^{-1}	0.11	0.06	0.15	0.23	0.37	0.3	0.08	0.13	0.11
Li_F	µg L^{-1}	0.25	0.35	0.1	0.15	0.6	0.9	0.2	0.2	0.15
Lu_F	µg L^{-1}	<0.01	<0.01	<0.01	<0.01	<0.01	<0.01	<0.01	<0.01	<0.01
Mn_F	µg L^{-1}	42.2	39.1	142	80.3	167	252	35.4	133	182
Mo_F	µg L^{-1}	0.1	0.4	0.1	<0.05	<0.05	0.15	<0.05	0.05	0.15

Variable	**Unit**	**Site**								
		MB1	**MB1**	**MB2**	**MB2**	**MB4**	**MB4**	**Bore 1h**	**MB12**	**MB12**
		surface	**depth**	**surface**	**depth**	**surface**	**depth**		**surface**	**depth**
		19-Jul	**19-Jul**	**19-Jul**	**19-Jul**	**18-Jul**	**18-Jul**	**21-Jul**	**22-Jul**	**22-Jul**
Nb_F	µg L^{-1}	<0.02	<0.02	<0.02	<0.02	<0.02	<0.02	<0.02	<0.02	<0.02
Nd_F	µg L^{-1}	0.17	0.09	0.19	0.3	0.58	0.46	0.13	0.2	0.13
Ni_F	µg L^{-1}	2.87	5.23	3	1.71	4.28	8.45	0.07	5.32	8.81
Os_F	µg L^{-1}	<0.1	<0.1	<0.1	<0.1	<0.1	<0.1	<0.1	<0.1	<0.1
Pb_F	µg L^{-1}	0.03	0.02	0.04	0.02	0.04	0.03	0.01	0.21	0.34
Pd_F	µg L^{-1}	<0.05	<0.05	<0.05	<0.05	<0.05	<0.05	<0.05	<0.05	<0.05
Pr_F	µg L^{-1}	0.03	0.03	0.04	0.07	0.13	0.09	0.03	0.05	0.03
Rb_F	µg L^{-1}	0.87	0.75	2.23	1.3	1.16	1.59	1.19	3.34	2.7
Re_F	µg L^{-1}	<0.01	<0.01	0.02	0.01	0.06	0.07	0.01	<0.01	0.01
Sb_F	µg L^{-1}	0.4	0.5	0.3	0.1	<0.05	0.1	<0.05	0.45	<0.05
Sc_F	µg L^{-1}	<0.05	<0.05	0.05	0.05	0.05	0.1	<0.05	0.1	0.05
Se_F	µg L^{-1}	<0.2	<0.2	<0.2	<0.2	<0.2	<0.2	<0.2	<0.2	<0.2
Sm_F	µg L^{-1}	0.04	0.02	0.04	0.08	0.1	0.07	0.03	0.04	0.04
Sn_F	µg L^{-1}	<0.1	<0.1	<0.1	<0.1	<0.1	<0.1	<0.1	<0.1	<0.1
Sr_F	µg L^{-1}	10.3	3.82	6.81	7.13	7.89	14	4.38	10.8	9.66
Ta_F	µg L^{-1}	<0.05	<0.05	<0.05	<0.05	<0.05	<0.05	<0.05	<0.05	<0.05
Tb_F	µg L^{-1}	<0.01	<0.01	<0.01	<0.01	0.01	<0.01	<0.01	<0.01	<0.01
Te_F	µg L^{-1}	<0.1	<0.1	<0.1	<0.1	<0.1	<0.1	<0.1	<0.1	<0.1
Th_F	µg L^{-1}	0.02	0.02	0.04	0.03	<0.01	<0.01	<0.01	0.03	0.03
Ti_F	µg L^{-1}	<2	<2	<2	<2	<2	<2	<2	<2	<2
Tl_F	µg L^{-1}	<0.01	<0.01	<0.01	<0.01	<0.01	<0.01	<0.01	<0.01	<0.01
Tm_F	µg L^{-1}	<0.01	<0.01	<0.01	<0.01	<0.01	<0.01	<0.01	<0.01	<0.01
U_F	µg L^{-1}	0.027	0.005	0.087	0.089	0.058	0.02	0.162	0.08	0.077
V_F	µg L^{-1}	1.15	4.3	1.9	2.55	4.15	7.15	0.6	1.55	1.35
W_F	µg L^{-1}	<0.05	<0.05	<0.05	<0.05	0.1	<0.05	<0.05	<0.05	<0.05
Y_F	µg L^{-1}	0.12	0.06	0.12	0.2	0.33	0.26	0.08	0.12	0.09
Yb_F	µg L^{-1}	<0.01	<0.01	<0.01	0.02	0.03	0.02	<0.01	0.02	<0.01
Zn_F	µg L^{-1}	187	46.7	7.3	3.1	7.6	14.4	0.7	7.1	21.5
Zr_F	µg L^{-1}	0.15	<0.05	0.1	0.15	<0.05	<0.05	<0.05	0.1	0.15
Filtered Cations										
Ca_F	mg L^{-1}	1.2	0.4	0.7	0.9	0.6	1.2	1.4	1.6	1.8
Mg_F	mg L^{-1}	1.8	0.7	1.3	1.5	12.8	10.7	2	1.6	2.4
Na_F	mg L^{-1}	0.2	0.2	0.3	0.3	0.4	0.6	0.3	0.6	0.3
K_F	mg L^{-1}	1.5	1.5	1.5	1.2	13.7	13.9	2.9	1.4	1.5
Total Metals										
Ag_T	µg L^{-1}	<0.05	<0.05	<0.05	<0.05	<0.05	<0.05	<0.05	<0.05	<0.05
Al_T	µg L^{-1}	1840	25500	2460	5280	4880	292000	75.3	263	269
As_T	µg L^{-1}	0.25	0.8	0.4	0.45	0.35	5.6	0.15	0.2	0.45
Au_T	µg L^{-1}	<0.01	0.05	<0.01	<0.01	<0.01	0.04	<0.01	<0.01	<0.01

Variable	Unit	Site								
		MB1	MB1	MB2	MB2	MB4	MB4	Bore 1h	MB12	MB12
		surface	depth	surface	depth	surface	depth		surface	depth
		19-Jul	19-Jul	19-Jul	19-Jul	18-Jul	18-Jul	21-Jul	22-Jul	22-Jul
B_T	µg L^{-1}	10	14.5	10	11.5	24	43	10.5	10	11
Ba_T	µg L^{-1}	32.2	121	22.6	31.6	80	1100	8.14	17.4	12.6
Be_T	µg L^{-1}	0.1	1.15	0.1	0.25	0.45	31.5	<0.05	<0.05	<0.05
Bi_T	µg L^{-1}	<0.01	0.21	<0.01	0.02	0.02	0.83	<0.01	<0.01	<0.01
Br_T	µg L^{-1}	31	32	30	32	173	282	17	16	20
Cd_T	µg L^{-1}	0.06	0.1	<0.02	<0.02	<0.02	0.58	<0.02	<0.02	<0.02
Ce_T	µg L^{-1}	2.96	29.5	2.31	5.8	7.1	439	0.3	0.6	0.54
Co_T	µg L^{-1}	2.03	11.6	2.78	3.37	15.9	114	0.14	3.11	3.44
Cr_T	µg L^{-1}	7.7	234	10.8	17.8	10.8	433	0.4	2	4.2
Cs_T	µg L^{-1}	0.13	1.91	0.25	0.5	0.41	18.5	0.05	0.06	0.06
Cu_T	µg L^{-1}	1.62	23.5	1.48	3.34	4.08	206	0.4	0.26	1.87
Dy_T	µg L^{-1}	0.16	1.45	0.11	0.27	0.34	23.2	0.02	0.04	0.03
Er_T	µg L^{-1}	0.07	0.6	0.04	0.11	0.16	10.2	<0.01	0.02	0.02
EU_T	µg L^{-1}	0.06	0.55	0.04	0.1	0.14	8.75	<0.01	0.01	0.01
Fe_T	µg L^{-1}	3200	11700	5050	5300	14800	85100	1800	4450	7300
Ga_T	µg L^{-1}	0.61	9.01	0.91	1.83	1.59	100	0.02	0.09	0.11
Gd_T	µg L^{-1}	0.23	2.11	0.16	0.37	0.52	34.7	0.02	0.06	0.05
Hf_T	µg L^{-1}	<0.01	0.03	<0.01	<0.01	<0.01	0.47	<0.01	<0.01	<0.01
Hg_T	µg L^{-1}	<0.02	0.02	<0.02	<0.02	<0.02	0.28	<0.02	<0.02	<0.02
Ho_T	µg L^{-1}	0.02	0.25	0.02	0.04	0.06	4.18	<0.01	<0.01	<0.01
I_T	µg L^{-1}	5	5	5	5	30	45	<5	<5	<5
In_T	µg L^{-1}	<0.01	0.02	<0.01	<0.01	<0.01	0.33	<0.01	<0.01	0.02
La_T	µg L^{-1}	1.4	14.3	1.17	2.88	3.26	195	0.1	0.24	0.25
Li_T	µg L^{-1}	1.35	16	1.8	3.9	3.35	197	0.3	0.45	0.35
Lu_T	µg L^{-1}	<0.01	0.06	<0.01	<0.01	0.02	1.02	<0.01	<0.01	<0.01
Mn_T	µg L^{-1}	56.6	193	150	91.3	173	640	36.2	130	182
Mo_T	µg L^{-1}	0.2	2.8	0.2	0.15	0.25	3.9	<0.05	0.1	0.2
Nb_T	µg L^{-1}	<0.02	0.08	0.02	0.02	0.02	0.48	<0.02	<0.02	<0.02
Nd_T	µg L^{-1}	1.34	13.3	0.93	2.51	3.34	203	0.17	0.3	0.23
Ni_T	µg L^{-1}	5.97	134	7.48	9.39	9.75	220	0.18	5.71	10.1
Os_T	µg L^{-1}	<0.1	<0.1	<0.1	<0.1	<0.1	<0.1	<0.1	<0.1	<0.1
Pb_T	µg L^{-1}	0.97	17.4	0.85	1.49	1.96	78.8	0.36	0.81	0.74
Pd_T	µg L^{-1}	<0.05	<0.05	<0.05	<0.05	<0.05	<0.05	<0.05	<0.05	<0.05
Pr_T	µg L^{-1}	0.34	3.4	0.25	0.62	0.81	50.8	0.04	0.07	0.06
Rb_T	µg L^{-1}	1.81	10.3	3.37	4.03	2.92	76.7	1.09	3.37	2.72
Re_T	µg L^{-1}	<0.01	<0.01	0.02	0.02	0.1	0.88	<0.01	<0.01	0.02
Sb_T	µg L^{-1}	0.35	0.5	0.3	0.15	<0.05	0.05	<0.05	0.4	<0.05
Sc_T	µg L^{-1}	0.45	4.75	0.5	1.15	1.15	73	0.1	0.15	0.15
Se_T	µg L^{-1}	<0.2	1	<0.2	<0.2	0.4	18.2	<0.2	<0.2	<0.2

Variable	Unit	Site								
		MB1 surface 19-Jul	**MB1 depth 19-Jul**	**MB2 surface 19-Jul**	**MB2 depth 19-Jul**	**MB4 surface 18-Jul**	**MB4 depth 18-Jul**	**Bore 1h 21-Jul**	**MB12 surface 22-Jul**	**MB12 depth 22-Jul**
Sm_T	µg L^{-1}	0.28	2.61	0.18	0.48	0.61	40.8	0.03	0.06	0.06
Sn_T	µg L^{-1}	0.1	0.2	<0.1	0.1	<0.1	0.2	<0.1	<0.1	<0.1
Sr_T	µg L^{-1}	12.5	19.2	9.02	9.49	8.86	55.9	4.54	10.5	9.8
Ta_T	µg L^{-1}	<0.05	<0.05	<0.05	<0.05	<0.05	0.05	<0.05	<0.05	<0.05
Tb_T	µg L^{-1}	0.03	0.27	0.02	0.05	0.07	4.43	<0.01	<0.01	<0.01
Te_T	µg L^{-1}	<0.1	<0.1	<0.1	<0.1	<0.1	0.1	<0.1	<0.1	<0.1
Th_T	µg L^{-1}	0.15	1.55	0.33	0.71	0.51	22.6	<0.01	0.05	0.1
Ti_T	µg L^{-1}	8	36	10	16	14	102	<2	<2	2
Tl_T	µg L^{-1}	<0.01	0.06	0.01	0.02	0.01	0.6	<0.01	<0.01	<0.01
Tm_T	µg L^{-1}	<0.01	0.08	<0.01	0.01	0.02	1.29	<0.01	<0.01	<0.01
U_T	µg L^{-1}	0.187	1.42	0.237	0.502	0.643	39.5	0.227	0.116	0.14
V_T	µg L^{-1}	4.25	48.5	4.8	8.6	14.5	787	0.65	1.95	2.2
W_T	µg L^{-1}	0.05	0.2	<0.05	<0.05	0.8	0.45	<0.05	<0.05	<0.05
Y_T	µg L^{-1}	0.73	6.66	0.45	1.11	1.65	110	0.1	0.17	0.17
Yb_T	µg L^{-1}	0.05	0.48	0.04	0.07	0.11	7.39	0.01	0.02	0.01
Zn_T	µg L^{-1}	334	328	10.4	6.3	9.4	118	23.7	7.2	22.9
Zr_T	µg L^{-1}	0.15	0.65	0.15	0.25	0.15	13.5	<0.05	0.05	0.15
Total cations										
Ca_T	mg L^{-1}	1.4	1.5	0.8	1.1	0.7	2.8	1.4	1.6	1.8
Mg_T	mg L^{-1}	0.4	1	0.4	0.5	0.5	4.4	0.3	0.6	0.4
Na_T	mg L^{-1}	2	2.3	1.4	1.8	13.2	24.7	2	1.6	2.4
K_T	mg L^{-1}	1.5	1.6	1.5	1.3	13.6	14.5	2.9	1.4	1.5
Anions and Alkalinity										
Cl	mg L^{-1}	2.2	2.5	2.4	1.9	6.8	7.1	3.2	2.4	3
S_F[3]	mg L^{-1}	0.02	0.07	0.07	0.1	27.84	29.44	0.03	0.13	0.1
S_T	mg L^{-1}	0.17	0.63	0.1	0.17	29.94	41.05	0.1	0.13	0.07
Hydroxide (OH)	mg L^{-1}	<1	<1	<1	<1	<1	<1	<1	<1	<1
Bicarbonate (HCO3)	mg L^{-1}	10	5	7	7	2	5	14	13	13
Carbonate (CO3)	mg L^{-1}	<1	<1	<1	<1	<1	<1	<1	<1	<1
Total Alkalinity	mg L^{-1}	10	5	7	7	2	5	14	13	13
EC	µS cm^{-1}	31	20	26	26	224	237	42	40	42
pH	units	6.6	6.1	6.6	6.5	5.5	4.8	6.9	6.5	7

---

[3] Used conversion factor of 2.996 to recalculate for S as assumed not fully oxidised in groundwaters

Table A1.2 August water chemistry data. Blank cells indicate variable was not recorded for that site

Variable	**Unit**	**Site**						
		MB1	**MB2**	**MB3**	**MB4**	**MB6**	**MB7**	**MB12**
		16-Aug	**16-Aug**	**16-Aug**	**16-Aug**	**17-Aug**	**17-Aug**	**17-Aug**
Field EC	µS cm^{-1}	52.7	56.5	372.2	201.5	116.1	308.5	53.4
Field pH	units	5.85	6.17	5.56	5.12	5.85	5.28	6.39
Field Temperature	ºC	27.65	29.52	28.09	26.81	27.07	28.33	26.65
Filtered Metals								
Ag_F	µg L^{-1}	<0.05	<0.05	<0.05	<0.05	<0.05	<0.05	<0.05
Al_F	µg L^{-1}	29	23.6	59.3	87.7	119	25.4	31.8
As_F	µg L^{-1}	0.15	0.35	0.05	0.1	0.1	0.125	0.5
Au_F	µg L^{-1}	<0.01	<0.01	<0.01	<0.01	<0.01	<0.01	<0.01
B_F	µg L^{-1}	12	10	15.5	19.5	29	29	9.5
Ba_F	µg L^{-1}	7.9	9.88	109	35.8	14.8	52.2	13.4
Be_F	µg L^{-1}	<0.05	<0.05	<0.05	<0.05	<0.05	0.1	<0.05
Bi_F	µg L^{-1}	<0.01	<0.01	<0.01	<0.01	<0.01	<0.01	<0.01
Br_F	µg L^{-1}	19	37	155	167	136	120.5	13
Cd_F	µg L^{-1}	0.3	<0.02	<0.02	<0.02	<0.02	<0.02	<0.02
Ce_F	µg L^{-1}	0.15	0.43	0.52	0.5	1.24	1.64	0.21
Co_F	µg L^{-1}	1.51	2.7	0.66	3.06	0.46	12.25	0.84
Cr_F	µg L^{-1}	0.2	0.3	0.4	0.4	0.5	0.1	0.4
Cs_F	µg L^{-1}	0.02	0.05	0.02	0.01	<0.01	0.035	0.04
Cu_F	µg L^{-1}	4.26	0.26	0.15	0.07	0.16	0.1	0.11
Dy_F	µg L^{-1}	0.01	0.02	0.03	0.03	0.06	0.065	0.01
Er_F	µg L^{-1}	<0.01	0.01	0.03	0.02	0.03	0.045	<0.01
Eu_F	µg L^{-1}	<0.01	<0.01	0.02	0.02	0.02	0.035	<0.01
Fe_F	µg L^{-1}	1400	5550	8950	7800	862	156500	4400
Ga_F	µg L^{-1}	<0.01	<0.01	0.01	<0.01	0.01	<0.01	0.02
Gd_F	µg L^{-1}	0.01	0.03	0.05	0.07	0.1	0.14	0.03
Hf_F	µg L^{-1}	<0.01	<0.01	<0.01	<0.01	<0.01	<0.01	<0.01
Hg_F	µg L^{-1}	<0.02	<0.02	<0.02	<0.02	<0.02	<0.02	<0.02
Ho_F	µg L^{-1}	<0.01	<0.01	<0.01	<0.01	0.01	0.02	<0.01
I_F	µg L^{-1}	<5	10	30	20	25	37.5	<5
In_F	µg L^{-1}	<0.01	<0.01	<0.01	<0.01	<0.01	<0.01	<0.01
La_F	µg L^{-1}	0.06	0.32	0.17	0.19	0.52	0.7	0.08
Li_F	µg L^{-1}	0.35	0.05	0.45	0.55	0.2	1.15	0.2
Lu_F	µg L^{-1}	<0.01	<0.01	<0.01	<0.01	<0.01	<0.01	<0.01
Mn_F	µg L^{-1}	77.4	313	452	87.1	58.9	266	91.3
Mo_F	µg L^{-1}	<0.05	0.05	<0.05	<0.05	<0.05	<0.05	<0.05
Nb_F	µg L^{-1}	<0.02	<0.02	<0.02	<0.02	<0.02	<0.02	<0.02
Nd_F	µg L^{-1}	0.1	0.17	0.34	0.28	0.66	1.035	0.12
Ni_F	µg L^{-1}	1.56	0.97	0.22	0.74	0.34	3.565	0.16
Os_F	µg L^{-1}	<0.1	<0.1	<0.1	<0.1	<0.1	<0.1	<0.1

Variable	**Unit**	**Site**						
		MB1	**MB2**	**MB3**	**MB4**	**MB6**	**MB7**	**MB12**
		16-Aug	**16-Aug**	**16-Aug**	**16-Aug**	**17-Aug**	**17-Aug**	**17-Aug**
Pb_F	µg L^{-1}	2.21	0.96	0.13	0.19	0.15	0.09	0.2
Pd_F	µg L^{-1}	<0.05	<0.05	<0.05	<0.05	<0.05	<0.05	<0.05
Pr_F	µg L^{-1}	0.02	0.04	0.07	0.06	0.16	0.225	0.03
Rb_F	µg L^{-1}	1.73	2.88	1.93	0.84	0.75	1.63	2.18
Re_F	µg L^{-1}	<0.01	0.01	0.07	0.03	0.05	0.02	<0.01
Sb_F	µg L^{-1}	0.4	<0.05	<0.05	<0.05	<0.05	<0.05	<0.05
Sc_F	µg L^{-1}	0.05	<0.05	0.05	0.1	0.1	0.075	0.05
Se_F	µg L^{-1}	<0.2	<0.2	<0.2	0.2	<0.2	<0.2	<0.2
Sm_F	µg L^{-1}	0.02	0.05	0.06	0.06	0.14	0.17	0.02
Sn_F	µg L^{-1}	0.2	<0.1	<0.1	<0.1	<0.1	<0.1	<0.1
Sr_F	µg L^{-1}	9.23	7.35	15.3	4.25	2.66	8.53	8.06
Ta_F	µg L^{-1}	<0.05	<0.05	<0.05	<0.05	<0.05	<0.05	<0.05
Tb_F	µg L^{-1}	<0.01	<0.01	<0.01	<0.01	0.01	0.01	<0.01
Te_F	µg L^{-1}	<0.1	<0.1	0.1	<0.1	<0.1	<0.1	<0.1
Th_F	µg L^{-1}	0.02	0.04	0.02	0.03	0.05	<0.01	0.04
Ti_F	µg L^{-1}	<2	<2	<2	<2	<2	<2	<2
Tl_F	µg L^{-1}	<0.01	<0.01	<0.01	<0.01	<0.01	<0.01	<0.01
Tm_F	µg L^{-1}	<0.01	<0.01	<0.01	<0.01	<0.01	<0.01	<0.01
U_F	µg L^{-1}	0.026	0.076	0.062	0.065	0.11	0.0375	0.034
V_F	µg L^{-1}	0.5	1	1.4	1.95	2.35	1.05	1
W_F	µg L^{-1}	<0.05	<0.05	<0.05	<0.05	<0.05	<0.05	<0.05
Y_F	µg L^{-1}	0.07	0.11	0.17	0.17	0.37	0.46	0.07
Yb_F	µg L^{-1}	<0.01	<0.01	0.02	0.02	0.03	0.045	<0.01
Zn_F	µg L^{-1}	92.4	12.7	7.1	13.9	1.8	10.8	5.7
Zr_F	µg L^{-1}	0.1	0.1	0.05	0.1	0.15	<0.05	0.1
Filtered Cations								
Ca_F	mg L^{-1}	1.3	1.6	1.1	0.3	0.2	0.8	1.3
Mg_F	mg L^{-1}	1.8	2	29.3	8.9	7.8	16.45	1.9
Na_F	mg L^{-1}	1.8	1.5	18.8	14.2	12.1	12.8	1.3
K_F	mg L^{-1}	1.5	0.4	1.2	0.3	0.2	0.4	0.5
Total Metals								
Ag_T	µg L^{-1}	0.15	<0.05	<0.05	<0.05	<0.05	<0.05	<0.05
Al_T	µg L^{-1}	1880	156	287	1920	525	174.5	775
As_T	µg L^{-1}	0.35	0.4	0.1	0.1	0.1	0.175	0.45
Au_T	µg L^{-1}	<0.01	<0.01	<0.01	<0.01	<0.01	<0.01	<0.01
B_T	µg L^{-1}	13.5	10	16.5	20	30	29.5	9.5
Ba_T	µg L^{-1}	15.2	12.4	113	40.4	16.4	52.2	18
Be_T	µg L^{-1}	0.1	<0.05	<0.05	0.1	<0.05	0.1	0.05
Bi_T	µg L^{-1}	0.02	<0.01	<0.01	<0.01	<0.01	<0.01	<0.01
Br_T	µg L^{-1}	25	42	158	166	145	128	18

Variable	**Unit**	**Site**						
		MB1	**MB2**	**MB3**	**MB4**	**MB6**	**MB7**	**MB12**
		16-Aug	**16-Aug**	**16-Aug**	**16-Aug**	**17-Aug**	**17-Aug**	**17-Aug**
Cd_T	µg L^{-1}	0.58	<0.02	<0.02	<0.02	<0.02	<0.02	<0.02
Ce_T	µg L^{-1}	3.4	0.63	0.72	1.77	1.61	1.88	1.34
Co_T	µg L^{-1}	2.49	3.05	0.74	3.59	0.58	12.55	1.14
Cr_T	µg L^{-1}	2.3	0.4	0.6	1.3	0.8	0.25	1.3
Cs_T	µg L^{-1}	0.17	0.07	0.05	0.12	0.04	0.055	0.1
Cu_T	µg L^{-1}	11.3	0.27	0.3	0.86	0.46	0.145	0.69
Dy_T	µg L^{-1}	0.19	0.02	0.04	0.09	0.1	0.085	0.07
Er_T	µg L^{-1}	0.09	0.01	0.02	0.04	0.04	0.055	0.03
EU_T	µg L^{-1}	0.06	0.01	0.02	0.04	0.03	0.04	0.02
Fe_T	µg L^{-1}	6150	5800	9150	8450	976	16000	4700
Ga_T	µg L^{-1}	0.69	0.05	0.11	0.44	0.21	0.05	0.28
Gd_T	µg L^{-1}	0.25	0.04	0.07	0.15	0.13	0.15	0.1
Hf_T	µg L^{-1}	0.01	<0.01	<0.01	0.01	<0.01	0.005	<0.01
Hg_T	µg L^{-1}	<0.02	<0.02	<0.02	<0.02	<0.02	0.01	<0.02
Ho_T	µg L^{-1}	0.03	<0.01	<0.01	0.02	0.01	0.02	0.01
I_T	µg L^{-1}	<5	5	25	20	20	30	<5
In_T	µg L^{-1}	<0.01	<0.01	<0.01	<0.01	<0.01	0.005	<0.01
La_T	µg L^{-1}	1.58	0.33	0.27	0.79	0.71	0.815	0.59
Li_T	µg L^{-1}	1.65	0.15	0.7	1.25	0.5	1.25	0.75
Lu_T	µg L^{-1}	<0.01	<0.01	<0.01	<0.01	<0.01	0.005	<0.01
Mn_T	µg L^{-1}	94.1	332	453	88.7	62.6	269.5	97.5
Mo_T	µg L^{-1}	0.05	0.05	<0.05	<0.05	<0.05	0.025	<0.05
Nb_T	µg L^{-1}	<0.02	<0.02	<0.02	0.02	<0.02	0.01	<0.02
Nd_T	µg L^{-1}	1.49	0.23	0.46	0.89	0.84	1.115	0.65
Ni_T	µg L^{-1}	3.28	0.31	0.35	1.31	0.56	3.7	0.53
Os_T	µg L^{-1}	<0.1	<0.1	<0.1	<0.1	<0.1	0.05	<0.1
Pb_T	µg L^{-1}	74	1.76	0.91	1.41	0.55	0.2	0.96
Pd_T	µg L^{-1}	<0.05	<0.05	<0.05	<0.05	<0.05	0.025	<0.05
Pr_T	µg L^{-1}	0.38	0.06	0.1	0.21	0.2	0.265	0.15
Rb_T	µg L^{-1}	2.73	2.93	2.08	1.37	1	1.715	2.68
Re_T	µg L^{-1}	<0.01	0.02	0.08	0.04	0.06	0.02	<0.01
Sb_T	µg L^{-1}	0.6	<0.05	<0.05	<0.05	<0.05	<0.05	<0.05
Sc_T	µg L^{-1}	0.6	0.1	0.1	0.3	0.2	0.125	0.3
Se_T	µg L^{-1}	<0.2	<0.2	<0.2	<0.2	0.2	<0.2	<0.2
Sm_T	µg L^{-1}	0.31	0.05	0.11	0.18	0.15	0.195	0.13
Sn_T	µg L^{-1}	1.4	0.1	0.1	0.1	0.1	0.05	0.2
Sr_T	µg L^{-1}	11.5	8.88	15.6	5.09	2.85	8.65	8.98
Ta_T	µg L^{-1}	<0.05	<0.05	<0.05	<0.05	<0.05	<0.05	<0.05
Tb_T	µg L^{-1}	0.03	<0.01	<0.01	0.02	0.01	0.015	0.01
Te_T	µg L^{-1}	0.2	0.2	0.2	0.1	0.1	0.2	0.2

Variable	**Unit**	**Site**						
		MB1	**MB2**	**MB3**	**MB4**	**MB6**	**MB7**	**MB12**
		16-Aug	**16-Aug**	**16-Aug**	**16-Aug**	**17-Aug**	**17-Aug**	**17-Aug**
Th_T	µg L^{-1}	0.34	0.06	0.06	0.22	0.12	0.035	0.22
Ti_T	µg L^{-1}	10	<2	<2	16	6	4.5	2
Tl_T	µg L^{-1}	<0.01	<0.01	<0.01	<0.01	<0.01	<0.01	<0.01
Tm_T	µg L^{-1}	<0.01	<0.01	<0.01	<0.01	<0.01	<0.01	<0.01
U_T	µg L^{-1}	0.22	0.091	0.092	0.197	0.163	0.0485	0.145
V_T	µg L^{-1}	6.3	1.25	1.65	3.8	2.9	1.675	2.05
W_T	µg L^{-1}	1.1	<0.05	<0.05	0.2	<0.05	<0.05	<0.05
Y_T	µg L^{-1}	0.86	0.12	0.2	0.44	0.43	0.545	0.32
Yb_T	µg L^{-1}	0.07	<0.01	0.02	0.04	0.04	0.045	0.02
Zn_T	µg L^{-1}	186	15.2	10	28.8	3	11.7	10.2
Zr_T	µg L^{-1}	0.35	0.1	0.1	1.65	0.2	0.15	0.15
Total Cations								
Ca_T	mg L^{-1}	1.5	1.7	1.1	0.4	0.2	0.8	1.3
Mg_T	mg L^{-1}	1.9	2	29.4	9.2	8	16.55	1.9
Na_T	mg L^{-1}	1.8	1.5	19	14.4	12.2	12.9	1.3
K_T	mg L^{-1}	1.6	0.4	1.2	0.4	0.2	0.4	0.5
Anions and Alkalinity								
Cl	mg L^{-1}	3.2	2.1	8.2	7.2	7.9	5.9	2
S_F[4]	mg L^{-1}	0.13	0.03	45.73	18.49	5.01	35.55	0.13
S_T	mg L^{-1}	0.13	0.02	46.06	19.43	5.54	36.05	0.17
Hydroxide (OH)	mg L^{-1}	<1	<1	<1	<1	<1	<1	<1
Bicarbonate (HCO3)	mg L^{-1}	10	14	26	8	32	3	12
Carbonate (CO3)	mg L^{-1}	<1	<1	<1	<1	<1	<1	<1
Total Alkalinity	mg L^{-1}	10	14	26	8	32	3	12
EC	µS cm^{-1}	39	38	370	182	124	270	35
pH	units	6.1	6.4	6.1	5.6	6.3	5.45	6.5
Nutrients								
Total N	mg L^{-1}	0.88	0.5	0.31	0.64	0.34	0.205	0.6
NO2_N	mg L^{-1}	<0.005	<0.005	<0.005	<0.005	<0.005	<0.005	<0.005
NO3_N	mg L^{-1}	0.005	0.005	<0.005	<0.005	<0.005	<0.005	<0.005
NH3_N	mg L^{-1}	0.19	0.39	0.08	0.08	0.065	0.065	0.56
PO4_P	mg L^{-1}	<0.005	<0.005	<0.005	<0.005	<0.005	<0.005	<0.005
Total P	mg L^{-1}	0.04	0.015	0.015	0.025	0.02	0.02	0.02
Total and dissolved organic carbon								
TOC	mg L^{-1}	12.13	5.183	8.525	38.88	12.37	4.55	33.17
DOC	mg L^{-1}	6.35	4.908	6.867	33.15	10.62	3.962	31.14

---

[4] Used conversion factor of 2.996 to recalculate for S as assumed not fully oxidised in groundwaters

Appendix 2 – Results of Principal Components Analysis of water chemistry data

Key influential variables for each axis (ie eigenvector coefficients in 90th percentile highlighted in grey shading; eigenvector coefficients of COPCs bolded).

Table A2.1 Eigenvalues from PCA of all water chemistry data for all subsurface sites sampled in July and August

PC	Eigenvalues	%Variation	Cum.%Variation
1	45.3	41.2	41.2
2	28.9	26.2	67.4
3	8.02	7.3	74.7
4	6.21	5.6	80.4
5	4.99	4.5	84.9

Table A2.2 Eigenvectors (Coefficients in the linear combinations of variables making up PCs) from PCA of all water chemistry data for all subsurface sites sampled in July and August

Variable	PC1	PC2	PC3	PC4	PC5
Log(Al_F)	0.050	0.049	0.233	0.072	0.105
Log(As_F)	-0.048	-0.064	-0.150	0.119	0.138
Log(B_F)	-0.062	0.157	0.049	-0.037	-0.026
Log(Ba_F)	-0.061	0.144	-0.080	-0.026	0.078
Log(Be_F)	-0.100	0.100	-0.123	0.020	-0.102
Log(Br_F)	-0.059	0.159	0.060	-0.028	0.052
Log(Ce_F)	-0.028	0.170	-0.006	0.063	-0.032
Log(Co_F)	-0.068	0.078	-0.163	-0.030	-0.060
Log(Cr_F)	-0.008	-0.079	0.071	0.127	0.203
Log(Cs_F)	-0.019	-0.024	-0.316	0.046	0.014
Log(Cu_F)	-0.062	-0.088	0.016	-0.229	0.041
Log(Dy_F)	-0.011	0.163	-0.024	0.101	0.003
Log(Er_F)	-0.025	0.174	0.011	0.044	-0.019
Log(Fe_F)	-0.028	0.118	-0.218	0.010	0.077
Log(Ga_F)	0.045	-0.047	0.009	0.125	0.189
Log(Gd_F)	-0.028	0.167	0.017	0.116	-0.052
Log(Ho_F)	-0.002	0.143	-0.034	-0.020	-0.215
Log(I_F)	-0.055	0.167	0.004	-0.022	0.055
Log(La_F)	-0.022	0.161	-0.033	0.066	-0.016
Log(Li_F)	-0.077	0.107	-0.003	-0.122	-0.157
Log(Mn_F)	**-0.019**	**0.101**	-0.229	-0.058	0.168
Log(Mo_F)	-0.068	-0.106	-0.032	0.089	0.008
Log(Nd_F)	-0.034	0.172	-0.006	0.047	-0.051
Log(Ni_F)	-0.081	-0.017	-0.117	0.038	-0.111
Log(Pb_F)	0.049	0.000	-0.054	-0.271	0.166
Log(Pr_F)	-0.034	0.169	0.003	0.065	-0.064

Variable	**PC1**	**PC2**	**PC3**	**PC4**	**PC5**
Log(Rb_F)	0.039	-0.019	-0.285	-0.025	0.168
Log(Re_F)	-0.056	0.138	0.050	0.058	0.157
Log(Sb_F)	-0.039	-0.127	0.036	-0.040	-0.110
Log(Sc_F)	-0.036	0.100	0.045	-0.016	0.135
Log(Sm_F)	-0.019	0.166	0.001	0.083	-0.043
Log(Sn_F)	0.000	-0.057	0.030	-0.312	-0.040
Log(Sr_F)	-0.032	0.002	-0.256	-0.091	0.101
Log(Th_F)	0.063	-0.076	0.120	0.006	0.224
Log(U_F)	**0.091**	**0.056**	-0.005	0.157	0.138
Log(V_F)	-0.115	0.015	0.074	0.185	0.068
Log(Y_F)	-0.038	0.166	0.009	0.061	-0.050
Log(Yb_F)	-0.035	0.162	0.019	0.029	-0.043
Log(Zn_F)	-0.043	-0.069	-0.027	-0.210	-0.091
Log(Zr_F)	0.068	-0.065	0.095	0.010	0.193
Log(Cl_F)	-0.048	0.151	0.083	-0.070	0.065
Log(Ca_F)	0.025	-0.069	-0.286	-0.040	0.062
Log(Mg_F)	**-0.030**	**0.170**	-0.018	-0.069	0.065
Log(Na_F)	0.026	0.145	0.059	-0.192	0.085
Log(K_F)	-0.088	-0.049	-0.096	0.097	-0.023
Log(S_F)	**-0.058**	**0.162**	0.012	-0.066	0.038
Log(Al_T)	-0.105	-0.063	0.143	-0.075	-0.014
Log(As_T)	-0.116	-0.081	-0.111	0.044	0.068
Log(B_T)	-0.091	0.135	0.055	-0.047	-0.015
Log(Ba_T)	-0.134	0.045	-0.022	-0.010	0.033
Log(Be_T)	-0.145	-0.015	-0.004	0.023	-0.043
Log(Bi_T)	-0.137	-0.050	0.012	-0.008	0.000
Log(Br_T)	-0.077	0.147	0.062	-0.040	0.059
Log(Cd_T)	-0.100	-0.080	0.027	-0.201	-0.012
Log(Ce_T)	-0.145	-0.020	0.037	0.002	-0.018
Log(Co_T)	-0.122	0.029	-0.115	-0.014	-0.073
Log(Cr_T)	-0.119	-0.092	0.042	0.102	0.013
Log(Cs_T)	-0.138	-0.056	0.005	0.047	0.011
Log(Cu_T	-0.123	-0.088	0.048	-0.016	0.036
Log(Dy_T)	-0.144	-0.023	0.049	0.005	-0.015
Log(Er_T)	-0.146	-0.013	0.027	-0.013	-0.014
Log(Eu_T)	-0.146	-0.010	0.040	-0.007	-0.017
Log(Fe_T)	-0.058	0.047	-0.193	-0.107	-0.111
Log(Ga_T)	-0.131	-0.061	0.080	0.031	0.049
Log(Gd_T)	-0.146	-0.016	0.035	-0.003	-0.008
Log(Hf_T)	-0.133	-0.028	0.000	-0.037	0.092
Log(Hg_T)	-0.130	-0.012	-0.042	0.017	0.123
Log(Ho_T)	-0.145	-0.017	0.025	0.002	-0.041

Variable	**PC1**	**PC2**	**PC3**	**PC4**	**PC5**
Log(I_T)	-0.076	0.154	0.037	-0.011	0.010
Log(In_T)	-0.122	-0.030	-0.060	0.037	0.136
Log(La_T)	-0.144	-0.023	0.037	0.002	-0.019
Log(Li_T)	-0.144	-0.018	0.026	0.014	-0.035
Log(Lu_T	-0.139	-0.018	-0.022	0.037	0.052
Log(Mn_T)	**-0.077**	**0.058**	-0.197	-0.066	0.131
Log(Mo_T)	-0.118	-0.086	-0.024	0.111	-0.015
Log(Nb_T)	-0.139	-0.029	0.011	0.060	0.057
Log(Nd_T)	-0.145	-0.010	0.040	-0.003	-0.025
Log(Ni_T)	-0.122	-0.050	-0.033	0.063	-0.097
Log(Pb_T)	-0.103	-0.091	0.035	-0.166	0.074
Log(Pr_T)	-0.145	-0.013	0.038	-0.002	-0.026
Log(Rb_T)	-0.129	-0.057	-0.092	0.028	0.097
Log(Re_T)	-0.093	0.101	0.000	0.061	0.211
Log(Sb_T)	-0.023	-0.129	0.048	-0.057	-0.130
Log(Sc_T)	-0.139	-0.053	0.038	0.035	0.019
Log(Se_T)	-0.138	-0.010	0.005	0.044	0.070
Log(Sm_T)	-0.146	-0.014	0.035	-0.008	-0.007
Log(Sn_T)	-0.042	-0.083	0.090	-0.296	0.061
Log(Sr_T)	-0.113	-0.052	-0.152	-0.061	0.064
Log(Tb_T)	-0.144	-0.028	0.037	0.012	-0.034
Log(Te_T)	0.013	0.079	-0.069	-0.290	0.096
Log(Th_T)	-0.130	-0.049	0.052	0.006	0.094
Log(Ti_T)	-0.122	-0.028	0.135	0.013	-0.050
Log(Tl_T)	-0.137	-0.036	-0.009	0.075	0.054
Log(Tm_T)	-0.140	-0.023	-0.016	0.050	0.046
Log(U_T)	**-0.131**	**-0.052**	0.035	0.077	0.077
Log(V_T)	-0.144	-0.037	0.035	0.021	0.036
Log(W_T)	-0.096	-0.028	0.067	-0.164	-0.071
Log(Y_T)	-0.146	-0.015	0.034	-0.003	-0.023
Log(Yb_T)	-0.144	-0.008	0.052	-0.006	-0.030
Log(Zn_T)	-0.067	-0.105	0.022	-0.160	-0.121
Log(Zr_T)	-0.124	-0.008	0.081	-0.065	0.116
Log(Cl)	-0.047	0.151	0.084	-0.071	0.064
Log(Ca_T)	-0.039	-0.109	-0.242	-0.038	0.027
Log(Mg_T)	**-0.017**	**0.136**	0.031	-0.201	0.094
Log(Na_T)	-0.068	0.153	0.052	-0.043	0.052
Log(K_T)	-0.090	-0.049	-0.088	0.093	-0.022
Log(S_T)	**-0.071**	**0.149**	0.051	-0.050	-0.023
Log(HCO3)	0.078	-0.040	0.108	-0.030	0.295
Log(Total Alkalinity)	0.078	-0.040	0.108	-0.030	0.295
Log(EC)	-0.042	0.167	-0.018	-0.075	0.051

Table A2.3 Eigenvalues from PCA of filtered water chemistry data for all subsurface sites sampled in July and August

PC	Eigenvalues	%Variation	Cum.%Variation
1	20.1	43.0	43.0
2	6.91	14.8	57.8
3	4.44	9.5	67.4
4	3.37	7.2	74.6
5	3.25	7.0	81.5

Table A2.4 Eigenvectors (Coefficients in the linear combinations of variables making up PCs) from PCA of filtered water chemistry data for all subsurface sites sampled in July and August

Variable	PC1	PC2	PC3	PC4	PC5
Log(Al_F)	-0.026	-0.287	-0.052	-0.159	-0.161
Log(As_F)	0.051	0.187	0.178	-0.006	-0.269
Log(B_F)	-0.212	-0.010	-0.082	-0.074	0.039
Log(Ba_F)	-0.190	0.063	0.087	-0.058	0.000
Log(Be_F)	-0.173	0.229	-0.035	0.035	-0.019
Log(Br_F)	-0.204	-0.045	-0.048	-0.116	-0.019
Log(Ce_F)	-0.192	-0.036	0.023	0.006	-0.092
Log(Co_F)	-0.128	0.214	0.090	-0.204	-0.115
Log(Cr_F)	0.097	-0.043	0.001	-0.257	-0.362
Log(Cs_F)	0.010	0.270	0.257	0.196	0.000
Log(Cu_F)	0.069	0.131	-0.041	-0.320	0.167
Log(Dy_F)	-0.176	-0.046	0.082	0.039	-0.103
Log(Er_F)	-0.208	-0.062	0.014	0.057	-0.021
Log(Fe_F)	-0.126	0.106	0.223	0.019	-0.042
Log(Ga_F)	0.072	-0.084	0.130	-0.031	-0.221
Log(Gd_F)	-0.171	-0.044	-0.018	0.075	-0.109
Log(Ho_F)	-0.176	0.011	-0.046	0.062	0.079
Log(I_F)	-0.212	-0.019	0.014	-0.056	-0.008
Log(La_F)	-0.176	-0.025	0.056	0.011	-0.102
Log(Li_F)	-0.164	0.117	-0.152	-0.063	0.183
Log(Mn_F)	**-0.110**	**0.092**	0.284	-0.087	-0.016
Log(Mo_F)	0.094	0.182	-0.153	-0.117	-0.228
Log(Nd_F)	-0.191	-0.019	0.006	0.007	-0.056
Log(Ni_F)	-0.028	0.263	-0.056	-0.240	-0.212
Log(Pb_F)	0.028	-0.061	0.266	-0.326	0.218
Log(Pr_F)	-0.189	-0.025	-0.017	0.022	-0.073
Log(Rb_F)	0.038	0.118	0.427	-0.009	-0.012
Log(Re_F)	-0.140	-0.045	0.008	-0.030	-0.080
Log(Sb_F)	0.122	0.136	-0.167	-0.201	-0.026
Log(Sc_F)	-0.126	-0.051	0.083	-0.216	-0.084
Log(Sm_F)	-0.178	-0.047	0.017	0.015	-0.103

Log(Sn_F)	0.063	0.046	0.003	-0.250	0.393
Log(Sr_F)	-0.023	0.224	0.283	-0.114	0.045
Log(Th_F)	0.132	-0.210	0.101	-0.235	-0.177
Log(U_F)	**-0.021**	**-0.196**	0.237	0.190	-0.102
Log(V_F)	-0.049	0.070	-0.142	-0.083	-0.268
Log(Y_F)	-0.200	-0.022	-0.006	-0.011	-0.091
Log(Yb_F)	-0.205	-0.036	-0.009	-0.039	-0.046
Log(Zn_F)	0.054	0.159	-0.089	-0.334	0.096
Log(Zr_F)	0.111	-0.183	0.149	-0.222	-0.163
Log(Cl_F)	-0.193	-0.073	-0.060	-0.101	0.091
Log(Ca_F)	0.086	0.193	0.323	0.120	0.101
Log(Mg_F)	**-0.206**	**-0.040**	0.072	-0.044	0.089
Log(Na_F)	-0.149	-0.186	0.095	-0.135	0.228
Log(K_F)	0.007	0.256	-0.066	0.076	-0.084
Log(S_F)	**-0.215**	**-0.007**	-0.005	-0.102	0.055
Log(Hydroxide Alkalinity)	0.000	0.000	0.000	0.000	0.000
Log(Bicarbonate Alkalinity (HCO3)	0.098	-0.269	0.155	-0.056	0.030
Log(Carbonate Alkalinity (CO3)	0.000	0.000	0.000	0.000	0.000
Log(Total Alkalinity)	0.098	-0.269	0.155	-0.056	0.030
Log(EC)	-0.208	-0.016	0.045	-0.051	0.098